

Aus dem Institut
Center for Cardiovascular Research (CCR)
der Medizinischen Fakultät Charité – Universitätsmedizin Berlin

DISSERTATION

Angiotensin II type 2 receptor stimulation. A novel options of
therapeutic interference with the renin-angiotensin system in
myocardial infarction?

zur Erlangung des akademischen Grades
Doctor medicinae (Dr. med.)

vorgelegt der Medizinischen Fakultät
Charité – Universitätsmedizin Berlin

von

Aleksandra Grzesiak
aus Nysa, Polen

Gutachter:

1. Priv.-Doz. Dr. med. E. Kaschina
2. Prof. M. Larhed
3. Prof. Dr. sc. hum. P. Gohlke

Promotionsdatum: 22.06.2014

Acknowledgements

I would like to express my heartfelt gratitude to Prof. Thomas Unger for creating a highly motivating scientific environment, for lots of freedom but also the pressure he put on me. I am deeply grateful for his support. I have got the unique opportunity to work in his lab - it was an unforgettable experience.

It is difficult to overstate my gratitude to my supervisor, Dr. Elena Kaschina. It has been an honor to be her student. I appreciate all her contributions of time, ideas, and funding to make my MD experience productive and stimulating. Her wide knowledge and her logical way of thinking have been of great value for me.

The members of the Prof. Unger group have contributed immensely to my personal and professional time at CCR. The group has been a source of friendships as well as good advice and collaboration. I am deeply thankful to Dr. UM Steckelings, Dr. A. Foryst-Ludwig, M. Timm, F. Rompe, M. Sommerfeld, UR Kemnitz, C. Curato, P. Namsolleck, Dr. J. Li, M. Krikov, W. Altarche-Xifro, M. Schröder.

I would especially like to thank CARDIOVASC Fellows: Caterina, Bianca, Luca, Catarina, Valeria, Georg and to Marie, Svetlana, Friedrich, Ania, Wassim. I had a great time with you.

I gratefully acknowledge the funding sources that made my MD work possible. I was funded by the Marie Curie Early Stage Research Training Programme (CARDIOVASC). Special Thanks to Project Coordinator Prof. Patricia Ruiz Noppinger and Project Manager Dian Michel for creating a very special atmosphere and taking a great care of all Fellows.

Table of contents

1. Introduction	9
1.1 Renin Angiotensin Aldosterone System (RAAS)	9
1.2 Angiotensin 1 Receptor (AT1R)	12
1.3 Angiotensin 2 Receptor (AT2R)	15
1.3.1 Tissue Distribution of the AT2 Receptor	15
1.4 AT2 Receptor Signaling.....	16
1.4.1 AT2 Receptor Signaling via Phosphatase Activation	16
1.4.2 G-protein Coupling of AT2 Receptors.....	16
1.4.3 AT2 Receptor Signaling via Activation of the NO/cGMP System.....	16
1.4.4 Ceramides and Caspases	17
1.5 Functional Properties of the AT2 Receptor.....	18
1.6 Compound 21 (C21).....	19
2. Methods	21
2.1 Animals	21
2.2 Myocardial Infarction.....	21
2.3 Experimental Protocol	22
2.4 Transthoracic Doppler Echocardiography	23
2.4.1 M-mode Measurements.....	24
2.4.2 Doppler Measurements.....	24
2.5 Determination of Left Ventricular and Scar Volumes by Magnetic Resonance Imaging.....	28
2.6 Millar catheter	30
2.7 Plasma Monocyte-chemoattractant Protein-1 (MCP-1) and Myelo-peroxidase (MPO) ELISAs	32
2.8 Quantitative real-time RT-PCR (qPCR)	32
2.9 Western Blot Analysis	33
3. Materials	34
3.1 Substances and Chemicals.....	34
3.1.1 Drugs.....	35
3.2 Kits	36
3.3 Electrophoresis and Blot System	37
3.4 Centrifuges and Rotors	37
3.5 Microscope	37
3.6 Operation Equipment.....	37

3.7 Buffers.....	38
3.7.1 Protein extraction.....	38
3.7.2 Western Blot Buffers	38
3.7.3 Argarose-Gelelectrophorese-Buffer	39
3.8 Primers.....	39
4. Results	40
4.1 Basal Parameters	40
4.2 Magnetic Resonance Imaging	40
4.3 Hemodynamic Measurements (Millar catheter).....	42
4.4 Transthoracic Doppler Echocardiography.....	45
4.5 Inflammation Markers	51
4.6 Apoptosis Markers	54
4.7 Immunohistology	55
4.8 p44/42 MAPK, p38 MAPK.....	55
4.9 Hemodynamic Measurements Obtained in Animals with Severe Post-infarct Impairment of Cardiac Function (EF<35%).....	57
4.9.1 Millar Catheter	57
4.9.2 Transthoracic Doppler Echocardiography	58
5. DISCUSSION.....	60
5.1 Conclusion	63
5.2 Limitations	63
6. Clinical Relevance	64
7. References.....	65
8. CURRICULUM VITAE	71
9. Erklärung	72
10. Published Abstracts	73

Summary

Background

This study is the first to examine the effect of direct Ang II type 2 (AT2) receptor stimulation on post infarct cardiac function with the use of the novel nonpeptide AT2 receptor agonist compound 21 (C21).

Methods and Results

Myocardial infarction (MI) was induced in Wistar rats by permanent ligation of the left coronary artery. Treatment with C21 (0.01, 0.03, 0.3 mg/kg per day i.p) started 24 hours after MI and continued until euthanasia (7 days after MI). Infarct size was assessed by magnetic resonance imaging, and hemodynamic measurements were performed via transthoracic Doppler echocardiography and intracardiac Millar catheter. Cardiac tissues were analyzed for inflammation and apoptosis markers via immunoblotting and real-time reverse transcription polymerase chain reaction. C21 significantly improved systolic and diastolic ventricular function. Scar size was smallest in the C21-treated rats. In regard to underlying mechanisms, C21 diminished MI-induced Fas-ligand and caspase-3 expression in the peri-infarct zone, indicating an anti-apoptotic effect. Phosphorylation of the p44/42 and p38 mitogen-activated protein kinases, both involved in the regulation of cell survival, was markedly reduced after MI but almost completely restored by C21 treatment. Furthermore, C21 decreased MI-induced serum monocyte chemoattractant protein-1 and myeloperoxidase as well as cardiac interleukin-6, interleukin-1, and interleukin-2 expression, suggesting an anti-inflammatory effect.

Conclusions

Direct AT2 receptor stimulation may be a novel therapeutic approach to improve post-MI systolic and diastolic function by antiapoptotic and anti-inflammatory mechanisms.

Publications

Parts of this work have been published:

1. *Angiotensin II type 2 receptor stimulation. A novel options of therapeutic interference with the renin-angiotensin system in myocardial infarction?*

Kaschina E, Grzesiak A, Li J, Foryst-Ludwig A, Timm M, Rompe F, Sommerfeld M, Kemnitz UR, Curato C, Namsolleck P, Tschöpe C, Hallberg A, Alterman M, Hucko T, Paetsch I, Dietrich T, Schnackenburg B, Graf K, Dahlöf B, Kintscher U, Unger T, Steckelings UM.

Circulation Dec 2008; 118: 2523 – 2532

2. *Telmisartan prevents aneurysm progression in the rat by inhibiting proteolysis, apoptosis and inflammation.*

Kaschina E, Schrader F, Sommerfeld M, Kemnitz RU, Grzesiak A, Krikov M, Unger Th.

Journal of Hypertension Dec 2008; 26(12):2361-2373

3. *Estrogen receptor α are expressed in post-infarct cardiac c-kit⁺ cells and support cardiomyocytes.*

Brinckmann M, Kaschina E, Altarche-Xifró W, Timm M, Curato C, Grzesiak A, Dong J, Kappert K, Unger Th, Li J.

Journal of Molecular and Cellular Cardiology JMCC Jul 2009; 47(1):66-75

4. *Cardiac c-kit⁺AT2⁺ cell population is increased in response to ischemic injury and supports cardiomyocyte performance.*

Altarche-Xifró W, Curato C, Kaschina E, Grzesiak A, Slavic S, Dong J, Kappert K, Steckelings MU, Imboden H, Unger Th, Li J.

Stem cells Oct 2009;27(10):2488-97

5. *The past, present and future of angiotensin II type 2 receptor stimulation.*

Steckelings MU, Rompe F, Kaschina E, Namsolleck P, Grzesiak A, Funke-Kaiser H, Bader M, Unger Th.

Journal of Renin-Angiotensin-Aldosterone System Mar 2010;11(1):67-73

Prices:

Austin Doyle Award 2008 (World Meeting on Hypertension, Berlin, June 14-19, 2008)

Abbreviations

A	late filling velocity
ACE	Angiotensin converting enzyme
ACEI	Angiotensin converting enzyme inhibitor
Ang	Angiotensin
ARBs	Ang II receptor blockers
AT1R	Angiotensin II receptor type 1
AT2R	Angiotensin II receptor type 2
BW	body weight
C21	Compound 21
E	early filling velocity
ECG	Electrocardiography
EDT	deceleration time of the early filling wave
EF	Ejection fraction
FS	Fractional shortening
IL	Interleukin
i.p	intraperitoneally
i.v	intravenous
LV	left ventricle
LVEDP	LV end-diastolic pressure
LVIDd	left ventricular inner diameter in diastole
MAPK	mitogen-activated protein kinases
LVIDs	left ventricular inner diameter in systole
maxdP/dt	maximal peak rate of left ventricular pressure
MCP	monocyte-chemoattractant protein-1
MI	myocardial infarction
mindP/dt	minimal peak rate of left ventricular pressure
MPO	myelo-peroxidase
MRI	magnetic resonance imaging
RAAS	renin angiotensin aldosterone system
SHR	spontaneously hypertensive rat
VSMC	vascular smooth muscle cells
2D	two dimensional

Introduction

According to WHO estimates 16.7 million people around the globe die of cardiovascular diseases each year. This represents about 1/3 of all deaths globally.

By 2020 heart disease and stroke will become the leading cause of both death and disability worldwide, with the number of fatalities projected to increase to over 20 million a year and by 2030 to over 24 million a year (2004, American Heart Association).

Among the fatal consequences of ischemic heart disease is myocardial infarction. This thesis contains a study focusing on pharmacological protection against the consequences of myocardial ischemia.

The study is based on the finding that the Ang II receptor type 2 (AT2R) might be associated with an improved outcome after myocardial infarction.

1.1 Renin Angiotensin Aldosterone System (RAAS)

The RAAS is a major component in regulating blood pressure, electrolyte balance, and fluid volume homeostasis. It plays a pivotal role in the pathogenesis of hypertension, congestive heart failure, and diabetic nephropathy (Fig.1). Renin release from juxtaglomerular cells located in renal afferent arterioles begins the RAAS cascade (Fig. 2). Factors triggering renin release include reduced perfusion pressure, decreased sodium chloride delivery to the distal tubule, and the direct action of catecholamines on β 1-receptors occupying juxtaglomerular cells. After its release, it cleaves the decapeptide Ang I from circulating glycoprotein angiotensinogen. Ang I has minimal biological activity and serves as a substrate for plasma or tissue Angiotensin-converting enzyme (ACE). ACE cleaves a dipeptide sequence from Ang I to yield the octapeptide Ang II. Ang II exerts its physiological actions at numerous sites in the body, including vascular smooth muscle, adrenal cortex, kidneys, and brain. Consequently, it is a key regulator of blood pressure and extracellular volume. Briefly, Ang II-mediated vasoconstriction of efferent arterioles and increased epinephrine release from the adrenal medulla both contribute to elevating blood pressure. Ang II controls intravascular volume by promoting synthesis and release of aldosterone from the adrenal cortex, which increases

proximal tubular sodium reabsorption. Other effects are thirst stimulation, decreased renin secretion and increased antidiuretic hormone secretion from the central nervous system.

Circulating and locally generated Ang II exerts other non-haemodynamic effects, which have been implicated in the regulation of cardiac and vascular cell proliferation (de Gasparo et al., 2000). In particular, Ang II is a potent stimulator of hyperplasia and hypertrophy in vascular smooth muscle cells (VSMC) (Berk et al., 1989; Geisterfer et al., 1988), and contributes to the release of a number of growth factors, including platelet-derived growth factor, basic fibroblast growth factor and transforming growth factor (Naftilan et al., 1989), as well as to the activation of proto-oncogenes such as c-fos, c-myc and c-jun, which are known to influence cell replication and division (Taubman et al., 1989). Ang II may also participate in the development of atherosclerosis via the generation of reactive oxygen species acting as a proinflammatory mediator (Ruiz- Ortega et al., 2001).

These notions on the effects of the RAAS, together with the increasing evidence of its involvement in the pathophysiology of numerous dangerous clinical conditions, such as arterial hypertension, congestive heart failure, myocardial infarction, stroke, diabetes and renal failure, have led, in the past 20 years, to an unrelenting hunt for compounds able to block the actions of Ang II effectively.

Pharmacological inhibition of the RAAS can occur by blocking renin secretion, renin action, Ang II receptors, and by converting Ang I to Ang II. Clinical intervention in the RAAS was first achieved with the introduction of ACE inhibitors, developed in the 1970s and 1980s. Then, in the 1990s, the Ang II receptor blockers (ARBs), which are specific for AT1 receptor, were introduced. Both classes of drugs are now widely used in the treatment of hypertension, heart failure and diabetic nephropathy. In 2007 the renin inhibitor aliskiren was approved for the treatment of hypertension.

Renin secretion can be inhibited by beta-blockers acting on juxtaglomerular cell β -receptors and secretion by direct inhibitors. The ACE inhibitors halt formation of Ang II from Ang I by the converting enzyme. In addition, they block degradation of the potent vasodilator bradykinin and substance P. Despite the potential clinical benefits of bradykinin and substance P accumulation were postulated to be responsible for the cough associated with ACE inhibitors.

Ang II can be generated by other enzymes including cathepsin G, tissue plasminogen activator, chymostatin-sensitive angiotensin II generator enzyme, and chymase. Because ACE inhibitors may not provide complete suppression of Ang II generation, Ang II receptor blockade offers the advantage of inducing absolute inhibition of Ang II activity. Ang II receptors exist as subtype 1 (AT1) and subtype 2 (AT2), with AT1 being responsible for the Ang II-mediated effects described above (Fig. 2).

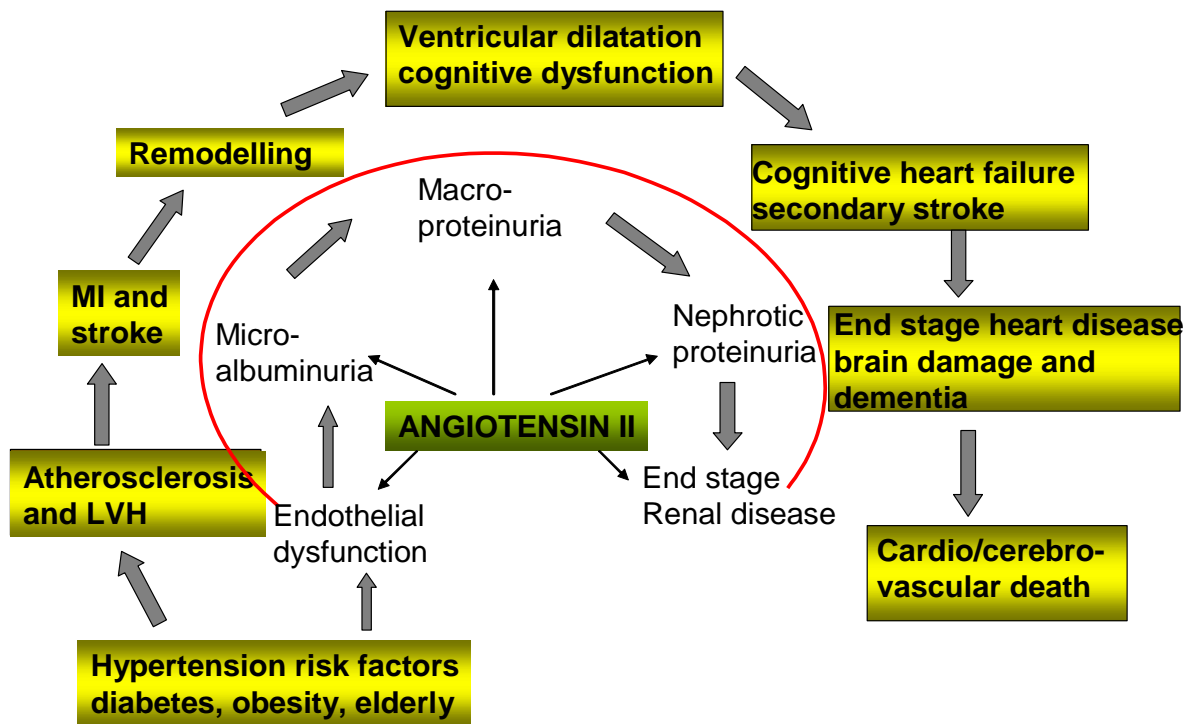


Figure 1: Cardiovascular disease: Role of Ang II in the cardiovascular continuum.

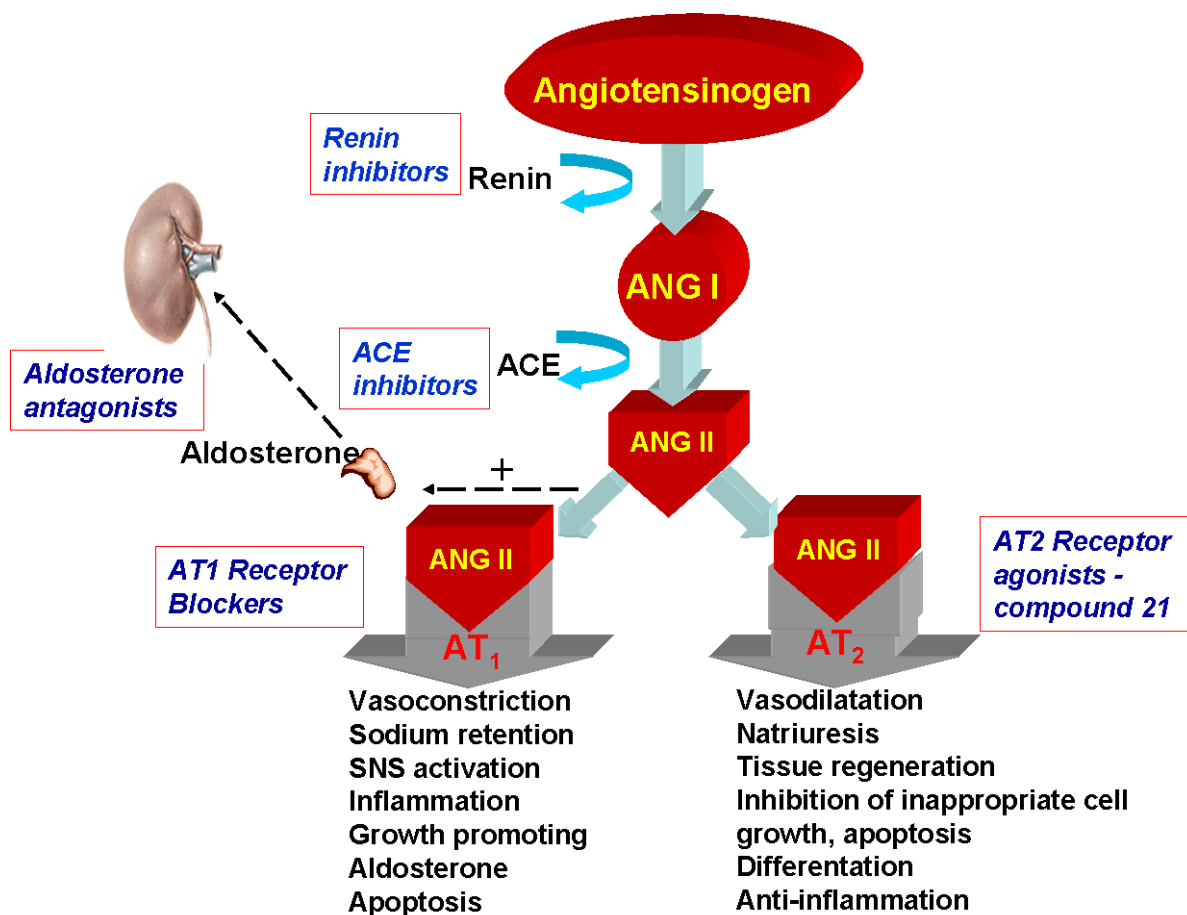


Figure 2: The RAAS cascade starts with angiotensinogen which is secreted by the liver. Ang I is cleaved from this substrate by renin which is produced in the kidney. Ang I is transformed by angiotensin- converting enzyme (ACE) to Ang II which binds to Ang II receptors (AT1R or AT2R), (modified from Kaschina et al., 2003).

1.2 Angiotensin 1 Receptor (AT1R)

The AT1R virtually mediates all known actions of Ang II in cardiovascular, renal, neuronal, endocrine, hepatic and other target cells. Altogether, these actions largely contribute to the homeostasis of arterial blood pressure, maintenance of electrolyte and water balance, thirst, hormone secretion, renal function and cellular growth (Fig.1).

AT1Rs are present in smooth muscle cells, endometrium, lung (the vasculature smooth muscle cells, macrophages and in the stroma underlying the airways epithelium), adrenals and brain. In the kidney, AT1R occurs primarily in glomerular mesangial cells (Gasparo et al., 1994), proximal tubular epithelia and the inner stripe of the outer medulla, the type 1 renomedullary interstitial cells (Zhuo et al., 1992). This underlines the importance of Ang II in the physiological regulation of glomerular filtration, renal cortical and medullary microcirculation, fluid and electrolyte balance, and in promoting renal cell proliferation and extracellular matrix synthesis in progressive renal disease (Navar et al., 1996). The distribution of AT1R in the adrenal gland located in the zona glomerulosa cells of the cortex and chromaffin cells of the medulla is consistent with the Ang II-mediated biosynthesis and release of aldosterone (Gigante et al., 1996) and catecholamines from the adrenal glands. Also, the distribution in heart and vessels is consistent with the known inotropic, chronotropic and vasomotor effects of Ang II (Zhuo et al., 1996). AT1R mediates Ang II-induced coronary vasoconstriction and long-term myocardial trophic effects implicated in the development of cardiac hypertrophy and remodeling processes. The AT1R is also present in the brain, on the presynaptic terminal of the dopamine neurons, highlighting the role of Ang II in the release of monoamine neurotransmitters at these sites (Allen et al., 1992). AT1-mediated effects of Ang II have been tightly linked to the development of atherosclerosis and thrombosis. Ang II, via AT1R, may promote development of atherosclerotic process at all stages of the disease. These actions are mediated partially by reactive oxygen species that inactivate endothelium-derived nitric oxide (Raij et al., 2001). A broad body of evidence indicates that AT1R activation leads to production of reactive oxygen species in the vessel wall, partially linked to activation of an NADH/NADPH oxidase in vascular cells (Griendling et al., 1994). Ang II activates the NADPH oxidase via AT1R activation through stimulation of intracellular signaling pathways, such as arachidonic acid metabolites. Beside these rapid effects, Ang II exerts long-term alterations of oxidative stress by enhancing the gene expression of proteins involved in the NADPH assembly and activation, such as the subunits gp91phox, p22phox, p47phox and p67phox (Fig. 3) (Touyz et al., 2002).

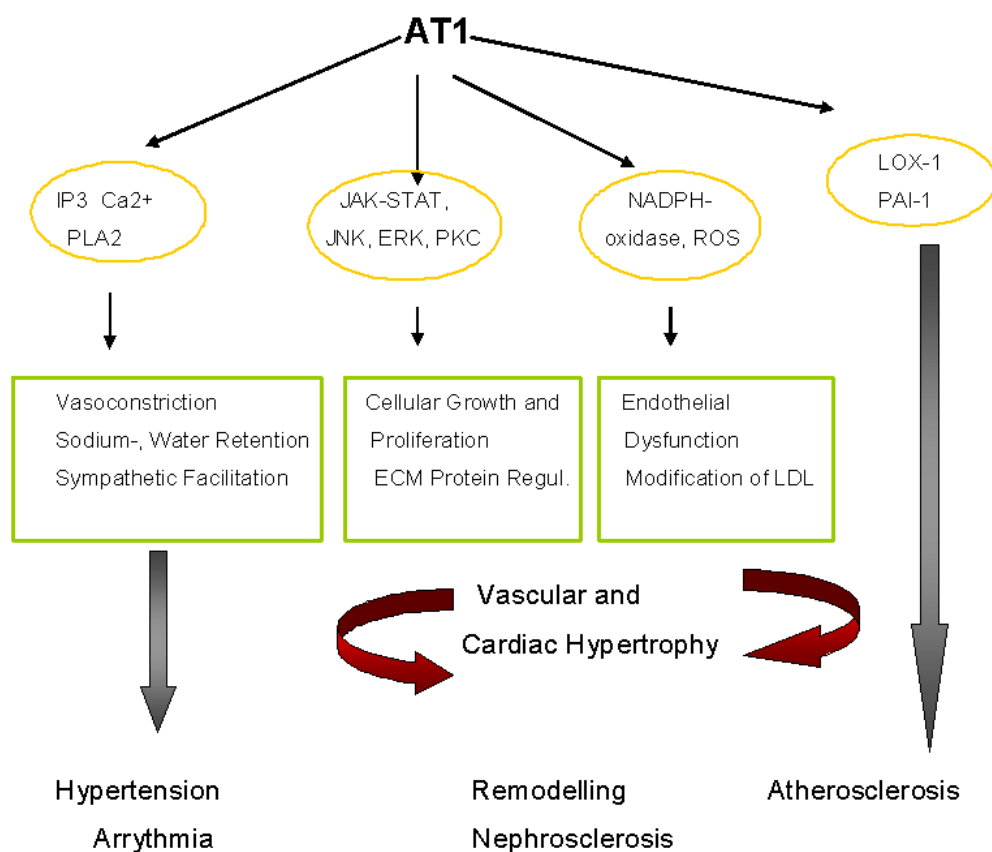


Figure 3: Summary of the major signaling pathway and effects of Ang II mediated by the AT1-R. IP3: inositol triphosphate; PLA2: phospholipase A2; JAK: Janus cytosolic protein kinase; STAT: signal transducers and activator transcription; ERK: extracellular signal-regulated kinase; PKC: protein kinase C; ROS: reactive oxygen species; ECM: extracellular matrix; LOX-1: lipoprotein receptor-1; PAI-1: plasminogen activator inhibitor type 1 (from Kaschina et al., 2003).

The Ang II-mediated increase in reactive oxygen species favours the attraction and adhesion of monocytes to the endothelium (Hsich et al., 1998), oxidation of low-density lipoprotein (LDL), uptake of oxidized LDL by macrophages and foam cell formation (Morawietz et al., 1999). The relationship between lipids and Ang II also works the other way around, in that hypercholesterolaemia, and particularly the exposure of VSMC to elevated LDL plasma concentrations, markedly augments AT1R expression by a stabilization of its mRNA. Touyz et al. (2001) have demonstrated in VSMC that Ang II via AT1R activates numerous MAP kinases by Src-dependent pathways. The activation of these kinases induces gene overexpression, resulting in altered growth signaling. Altogether these mechanisms are pathophysiologically relevant, since it has been demonstrated that both Angiotensin converting enzyme inhibitors (ACEI) and Ang II Receptor blockers (ARBs) reduce oxidative stress and reduce endothelial dysfunction, slowing the progression of atherosclerosis (Prasad et al., 2002).

1.3 Angiotensin 2 Receptor (AT2R)

1.3.1 Tissue Distribution of the AT2 Receptor

In foetal tissue, AT2R is the predominant subtype expressed, although this situation is rapidly reversed after birth with the AT1R becoming the dominant subtype in the adult (Matsubara et al., 1998; Horiuchi et al., 1999a; de Gasparo et al., 2000).

AT2R predominates in adult tissue only at particular sites including uterus, ovary, adrenal medulla as well as in distinct areas of the brain (Zhuo et al., 1995; de Gasparo et al., 2000; Roulston et al., 2003). At low levels it is expressed in coronary arteries, the vascular smooth muscles of the aorta and pulmonary arteries, and ventricular myocardium.

The AT2R gains particular prominence in the human heart. In both normal non-infarcted and hypertrophied human hearts, there is a predominance of AT2R binding sites in the myocardium (Brink et al., 1996; Matsubara, 1998; Wharton et al., 1998; de Gasparo et al., 2000). Even in studies that indicate that the AT2R is not the major subtype, there were approximately equal proportions of both AT2R and AT1R in non-failing human hearts (Tsutsumi et al., 1998).

Although the AT2R is usually expressed at low density in adult, it is up-regulated to different extents in pathological circumstances such as vascular injury, cardiac hypertrophy, myocardial infarction (Nio et al., 1995), cardiomyopathy and congestive heart failure (Matsubara et al., 1998). Interestingly, both in non-failing and explanted end-stage human heart, the AT2R population measured in a binding assay (65% of total Ang II receptor) is greater than AT1R, and there may be a correlation between the density of the AT2Rs and the severity of heart failure (Rogg et al., 1996). Wharton et al. (1998) also observed a significantly increased density

of high-affinity binding sites in endocardial, interstitial, perivascular, and infarcted regions of the ventricle of patients with end-stage ischemic heart disease or dilated cardiomyopathy, greater than in adjacent noninfarcted myocardium. The border zone between noninfarcted and infarcted myocardium was rich in microvessels with perivascular AT2Rs. Ohkubo et al. (1997) reported that in the heart of cardiomyopathic hamster, both AT1- and AT2Rs were increased during heart failure (153% and 72%, respectively). In human, the expression of the AT2R was markedly (3-fold) increased in patients with dilated cardiomyopathy at both protein and mRNA levels compared with patients with acute or well organized old myocardial infarction (Tsutsumi et al., 1998). In contrast, the AT1R expression was significantly down-regulated. The AT2R sites were highly localized in the interstitial region in the fibrotic areas where fibroblasts are present.

1.4 AT2 Receptor Signaling

1.4.1 AT2 Receptor Signaling via Phosphatase Activation

Up to now, three specific phosphatases could be identified, which are stimulated upon AT2R activation: mitogen-activated protein kinase phosphatase 1 (MKP-1) (Horiuchi et al., 1997), SH2 domain-containing phosphatase 1 (SHP-1) (Bedecs et al., 1997) and protein phosphatase 2A (PP2A) (Huang XC et al., 1995) and more may follow. Major action of AT2Rs is to counteract growth factor-induced cell proliferation and to induce apoptosis. Growth factors (including Ang II via the AT1R) mediate their growth promoting actions preferably via tyrosine-kinase receptors and several additional kinase-driven phosphorylation steps further “down” the respective signaling cascades. Extra-cellular signal-regulated kinases 1 and 2 (ERK 1/2) seem to play a key role in these phosphorylation cascades. The AT2R negatively cross-talks with these cascades by reversion of the phosphorylation steps through phosphatase activation. Most documented is the dephosphorylation and subsequent inhibition of ERK 1/2 as a result of AT2R activation, and all three AT2R-activated phosphatases (MKP- 1, SHP-1, and PP2A) seem to be involved (Horiuchi et al., 1997; Huang XC et al., 1995).

1.4.2 G-protein Coupling of AT2 Receptors

In some cases, AT2Rs are coupled to $G_{i\alpha 2}$ and $G_{i\alpha 3}$ proteins (Kang J et al., 1994). However, activation of the tyrosine phosphatase SHP-1 seems to depend on the $G\beta\gamma$ - independent constitutive association of GS with SHP-1 and the AT2R. In a non-activated state, SHP-1 is kept inactive through interaction of two SH2 domains, which are part of the SHP-1 molecule itself, with its catalytic domain. Upon ligand binding to the AT2R, SHP-1 dissociates from the receptor and is activated by removal of the self-constrain imposed by the SH2 domains.

1.4.3 AT2 Receptor Signaling via Activation of the NO/cGMP System

Activation of NO release with a subsequent increase in intracellular cGMP levels is one of very few – if not the only - signaling pathway(s), which are/is shared by AT1 and AT2Rs (Hannan RE et al., 2004). Despite a growing body of data on this topic, the AT2R/NO/cGMP cascade is not yet fully understood.

1.4.4 Ceramides and Caspases

Ceramides are de novo synthesized upon AT2R activation, probably mediating a pro-apoptotic stimulus via activation of caspase 3 (Gallinat S et al., 1999). Caspase 3 had previously been shown, too, to be upregulated via AT2Rs and to mediate apoptosis (Dimmeler S et al., 1997). Lehtonen et al. (1998) described the same pro-apoptotic pathway and provided further evidence for the assumption that AT2R-induced apoptosis depends on the de-novo synthesis of ceramides by showing that blockade of sphingolipid synthesis abolished AT2R-mediated programmed cell death, (Fig. 4).

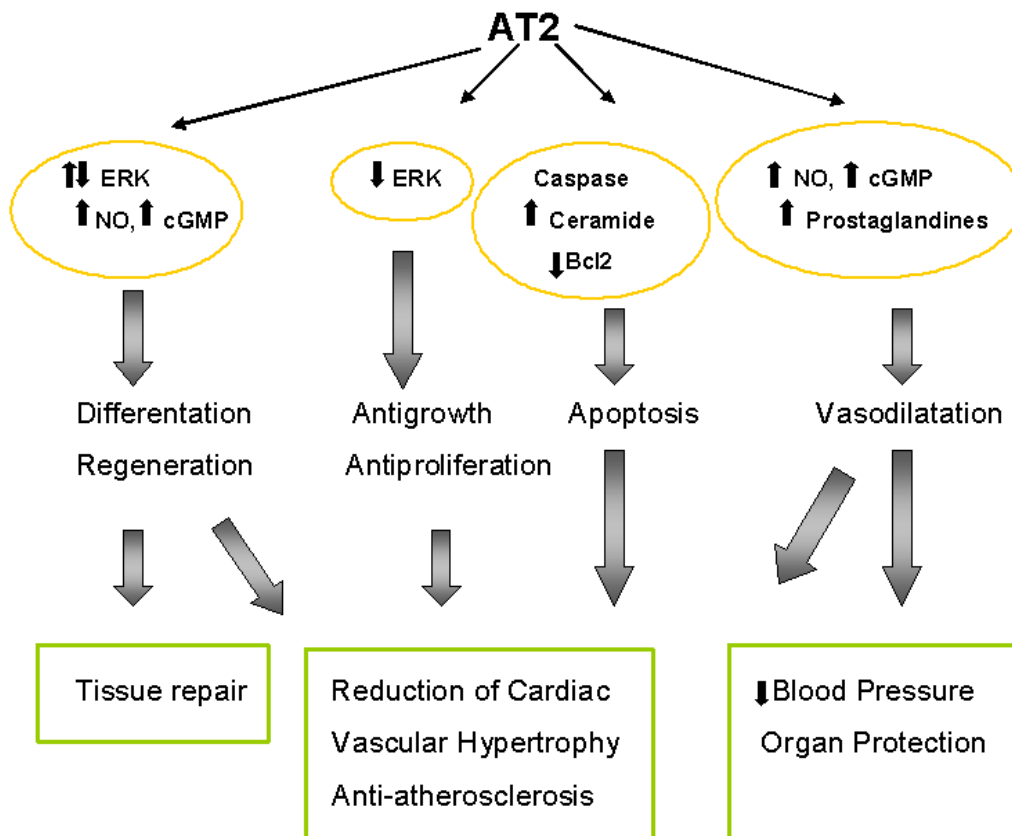


Figure 4: Summary of the major signalling pathway and effects of Ang II-mediated by the AT2-R. ERK: extracellular signal-regulated kinase; NO: nitric oxide; cGMP: cyclic guanosine monophosphate; Bcl2: B-cell leukaemia 2 protein; JNK: c-Jun N-terminal kinase (from Kaschina et al., 2003).

1.5 Functional Properties of the AT2 Receptor

Significant progress has been made lately in the elucidation of the functional properties of the AT2R. Physiologically, the AT2R appears to act as a modulator of complex biological programs involved in embryonic development, cell differentiation, apoptosis, regulation of renal function and blood pressure (de Gasparo M et al., 2000; Unger T et al., 1999; Carey RM et al., 2000). Moreover, the AT2R is involved in different pathophysiological processes such as cardiovascular remodeling following myocardial infarction and hypertension, heart failure and stroke, and it can be speculated that AT2R-mediated effects are even more apparent in pathological situations in which these receptors are upregulated. It seems that one major task of AT2Rs consists in a protective effect against an overstimulation of AT1Rs, and these opposing effects may occur beyond the level of the cell membrane receptor. For example, regression of cardiac fibrosis and vascular remodelling evoked by AT2Rs oppose the profibrotic AT1R-mediated action of Ang II (Wu L et al., 2002; Wu L et al., 2001). It has also been reported that vasodilatory effects of Ang II linked to the AT2R oppose the vasoconstrictor actions of Ang II-mediated by the AT1R (Carey RM et al., 2000). Furthermore, AT2Rs may play a role in pressure natriuresis, opposing the antinatriuretic effects of AT1Rs activation (Carey RM et al., 2000).

Studies to identify the role of the AT2R in (patho-) physiology have been conducted using diverse approaches which include the use of cultured cells, transgenic expression of AT2R, knockout mice lacking the AT2R and chronic administration of AT2R antagonist (PD123319). Animal studies directly addressing the role of the AT2R in myocardial infarction are controversial: while most studies claim that the AT2R stimulation improves post-infract cardiac function, others report either no effect on the outcome or even deterioration (Widdop et al., 2003).

Discrepancies noted between some of the rat studies may relate to the variety of experimental models that have been used, differences in drug doses, length of treatment, etc.

Myocardial infarction (MI) has also been produced in mice, but again with conflicting results that may relate to the different times examined after MI and/or strains. In the AT2R knockout strain which could not evoke a pro-hypertrophic/fibrotic response (Senbonmatsu et al., 2000; Ichihara et al., 2001), there was increased rupture immediately following MI although survival rate was not different from controls 6 weeks after MI (Ichihara et al., 2002). By contrast, in the AT2R knockout strain, which exhibited enhanced perivascular fibrosis (Akishita et al., 2000b), the survival rate was lower than that in controls 2 weeks after MI but without any difference in the incidence of rupture (Oishi et al., 2003).

Moreover, the MI-induced left ventricular enlargement and fibrosis seen in wild types was attenuated in one study (Ichihara et al., 2002) but enhanced in another (Oishi et al., 2003), in line with the contrasting pre-existing phenotypes. However, others have reported no differences in MI remodelling after 24 weeks (Xu et al., 2002). In addition, in mice with cardiac AT2R overexpression, left ventricular function was enhanced compared with wild

types, as assessed by magnetic resonance imaging techniques (Yang et al., 2002). Moreover, this left ventricular remodelling was preserved when measured invasively and noninvasively 28 days after myocardial infarction (Yang et al., 2002).

The inconsistency of data about AT2R actions may in part be due to the fact that detection and assignment of AT2R-mediated effects has always been difficult. AT2R-mediated effects had to be examined either by treatment of cells or animals with Ang II under concomitant AT1R-blockade which resulted in complex experimental protocols, or they were examined in genetically altered animals either over-expressing or lacking the AT2R. The only currently available pharmacological AT2R antagonist, PD 123319, lacks selectivity when applied at higher doses and has thus given rise to contradictory findings, especially when applied in vivo (Macari et al., 1993). An experimental tool to directly stimulate the AT2R under in vivo conditions was lacking until now.

In 2004, the synthesis of the first non-peptide AT2R agonist (Compound 21) was published (Wan et al., 2004), a compound which allows to specifically and selectively stimulate the AT2R in in vitro and in vivo settings. With a K_i of 0.4 nM for the AT2R and a $K_i > 10 \mu\text{M}$ for the AT1R, this substance possesses high selectivity for the AT2R.

The study presented here is the first to evaluate the role of the AT2R in post-MI cardiac function by direct AT2R stimulation in vivo using the non-peptide AT2R agonist compound 21 (C21). Myocardial infarction was induced in normotensive Wistar rats by permanent ligation of the left anterior descending artery. After a one week treatment period, scar volume was assessed by MRI and hemodynamic function by echocardiography and Millar catheter. In a first attempt to address the underlying mechanisms of C21 actions, markers of inflammation and apoptosis were determined in cardiac tissue and plasma. To obtain a first qualitative estimate of the effectiveness of C21, a group of animals was included which was treated with the AT1R-antagonist candesartan as a reference drug.

1.6 Compound 21 (C21)

There are several AT1R antagonists (candesartan, losartan, valsartan, telmisartan) which are used in the clinic for the treatment of hypertension. By contrast, only few selective AT2R agonists (used as research tools) were available before 2004, and they were all peptides e.g. CGP-42112. In 2004 Wan et al. described the first non-peptide, selective AT2R agonist, C21 (N-butyloxycarbonyl-3-(4-imidazol-1-ylmethylphenyl)-5-isobutylthiophene-2-sulphonamide). C21 was derived by transforming the drug-like but non-selective AT1R and AT2R agonist L-162313 into a selective AT2R agonist. The bioavailability after oral administration is 20-30% and the half life is estimated to be 4h in rat. The peptidomimetic C21 elicits a similar biological response as the endogenous peptide Ang II after selective activation of the AT2R (Wan et al., 2004).

C21 has been shown to induce neurite outgrowth in cell culture and increase duodenal mucosal alkalization in the rat via stimulation of MAPK and NO/cGMP signaling pathways (Wan et al., 2004). Our pioneer work published in 2008 (Kaschina et al.) triggered an explosion in AT2R research with C21. Bosnyak et al., (2010) established that C21 evoked vasorelaxation in mouse and SHR aorta or rat mesenteric arteries, and vasodepressor responses in conscious Spontaneously Hypertensive Rats (SHR), via AT2R stimulation. Krämer et al., (2010) reported that C21 significantly ameliorated uremic cardiomyopathy in experimental chronic kidney disease through antihypertrophic, anti-fibrotic and anti-inflammatory pathways. Furthermore, Lucinda et al., (2012) showed that direct AT2R stimulation with C21 significantly increased renal blood flow, without influencing arterial blood pressure and significantly increased sodium and water excretion. Fei Jing et al., (2012) observed that C21 enhances cognitive function in C57BL6 mice owing to an increase in cerebral blood flow, enhancement of hippocampal field-excitatory post-synaptic potential, and neurite outgrowth in hippocampal neurons. And just recently, Rehman et al.,(2012) noticed that C21 reduced vascular injury and myocardial fibrosis in stroke-prone SHR by reducing oxidative stress, collagen content, fibronectin, and inflammatory cell infiltration.

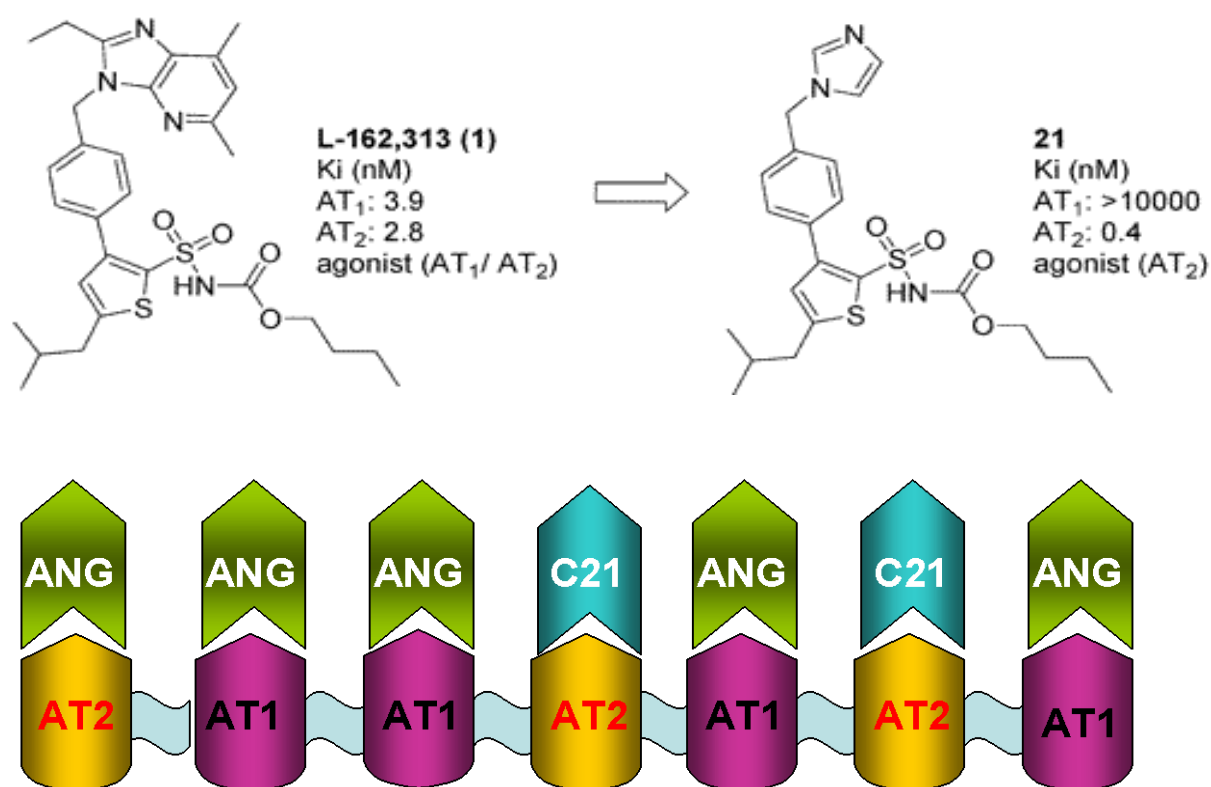


Figure 6: C21 the first selective, non- peptide Ang II AT2R agonist. C21 was derived from the prototype nonselective AT1/AT2R agonist L-162,313. ANG: Ang II; C21: compound 21.

Methods

2.1 Animals

Male normotensive Wistar rats (200-220g, HARLAN Winkelmann, Borchon, Germany) were kept in a SPF (specific pathogen free) barrier under standardized conditions with respect to temperature and humidity, and were housed on a 12h light/12h dark cycle in groups of 5 with food and water ad libitum. Animal housing, care, and applications of experimental procedures complied with the Guide for the Care and Use of Laboratory Animals of the State Government of Berlin, Germany.

Animals were randomly assigned to the following treatment groups comprising 8 animals each: vehicle treatment; treatment with C21 (0.01; 0.03; 0.3 mg/kg/day i.p.); treatment with C21 + PD123319 (0,03 mg/kg C21; 3 mg/kg PD123319); treatment with candesartan (0,2 mg/kg/day i.p.); treatment with C21+candesartan (0,03 mg/kg C21; 0,2 mg/kg/day candesartan). A low dose of candesartan (0,2 mg/kg/day) was chosen, because in prior experiments of our group, this dose had shown beneficial functional and cellular effects post-MI without affecting blood-pressure. Drugs were applied intraperitoneally (i.p.) starting 24 hours after myocardial infarction to allow for determination of ejection fraction after MI under untreated conditions. After 6 days of treatment, animals were sacrificed and plasma and hearts collected.

2.2 Myocardial Infarction

Rats were anesthetized with ketamin/xylazine (Sigma) 80 mg/10 mg/kg i.p., intubated and ventilated with a small-animal ventilator (Starling Ideal Ventilator, Harvard Apparatus) with room air at a rate of 75 cycles per minutes and a tidal volume of 3,5 ml.

A left lateral thoracotomy in the fourth or fifth intercostal space was performed, pericardium was removed, the heart was rapidly exteriorized, and a 6-0 silk suture was tightened around the proximal left anterior descending coronary artery. The muscle layer and skin were closed separately and the rats were allowed to recover. Sham-operated rats underwent the same surgical procedure with the exception of coronary ligation, (Fig. 7).

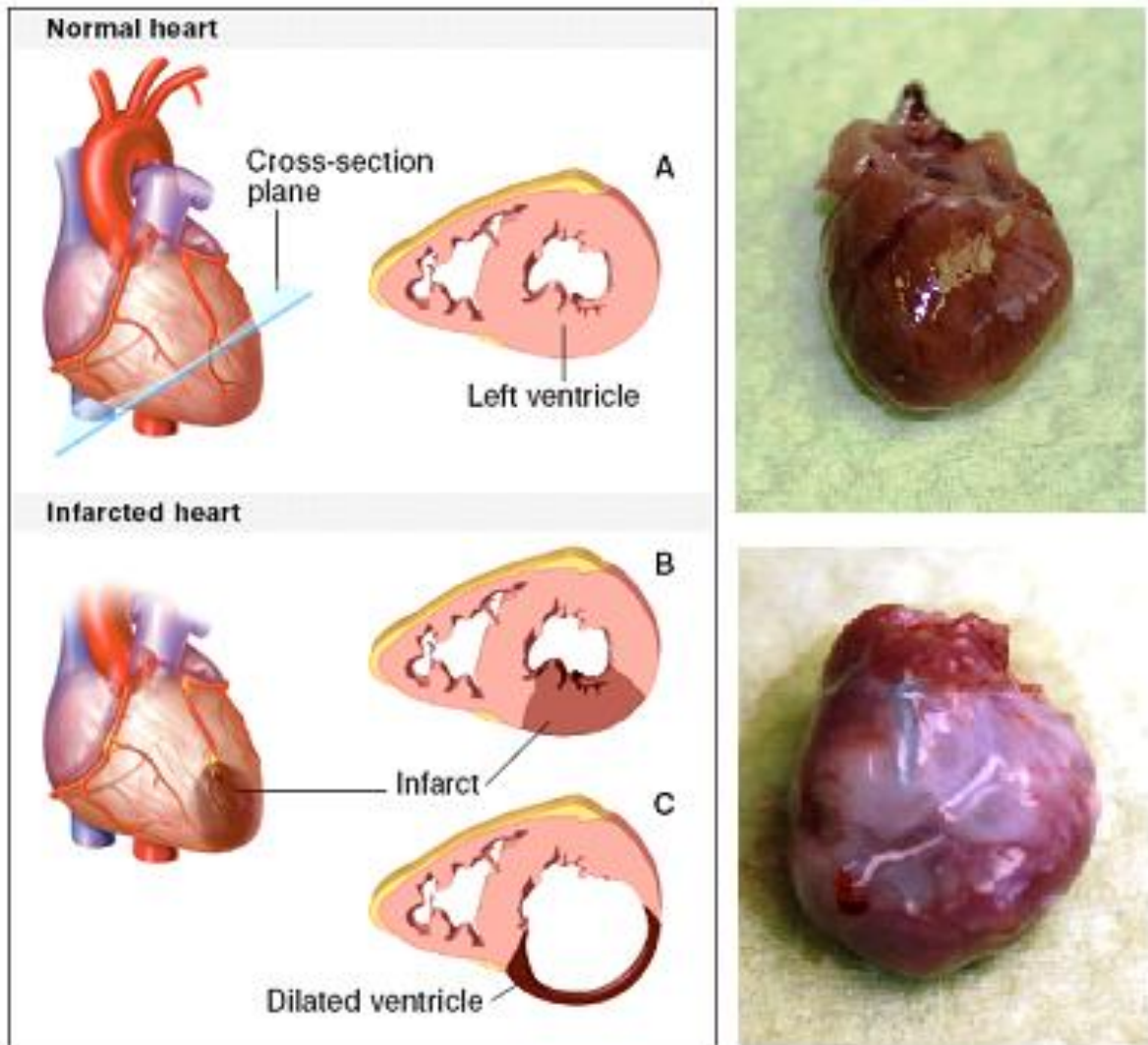


Figure 7: Surgical myocardial infarction model. A. Healthy heart. B, C Infarcted heart.

2.3 Experimental Protocol

Transthoracic Doppler echocardiography was performed 24 hours after MI to assess baseline cardiac function. With respect to these data and for better comparability of outcome between groups, rats were assigned to two different groups for later data analysis according to ejection fraction (EF). Those with $EF > 36\%$ were defined as having myocardial infarction with minor to moderate impairment of cardiac function; those with $EF \leq 35\%$ as having severe impairment of cardiac function. This procedure was applied to drug- treated and vehicle- treated animals alike and treatment and control groups were compared accordingly. Treatment of animals started 1 day after induction of MI and was continued until sacrifice (7 days post MI). Sham operated animals served as controls, (Fig. 8).

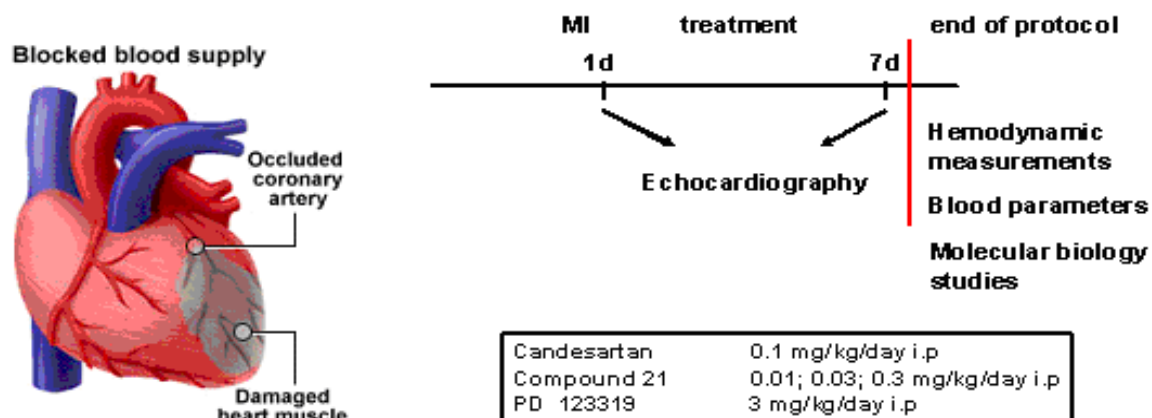


Figure 8: Experimental protocol.

2.4 Transthoracic Doppler Echocardiography

Echocardiography is an excellent real-time imaging technique with moderate spatial and temporal resolution. Its strength is the assessment of myocardial thickness, thickening, and motion at rest.

Transthoracic Doppler echocardiography was performed on days 1 and 7 after MI. Rats were anesthetized with 1,5% to 2% isoflurane in oxygen through a face mask. The chest was shaved and depilated, and the rats were placed on a heated platform in the supine position with all legs taped to ECG electrodes for heart rate monitoring.

Images were obtained by placing the transducer gently against the chest from below. A high-resolution imaging system Vevo 770 (VisualSonics Inc., Toronto) equipped with a 25 MHz single-crystal transducer with a focal length of 15mm, a frame rate of 40 Hz and the maximum field of view of 2D imaging 21x21mm were used, (Fig. 9). All data were transferred to a computer for offline analysis. Three measurements per heart were performed, averaged, and statistically analyzed.

2.4.1 M-mode Measurements

M-mode tracings were recorded from short-axis view of the LV at the level of the papillary muscles with two-dimensional image guidance through the anterior and posterior LV walls (Figure 11). To obtain a short-axis view transducer was gently applied to the mid upper left anterior chest wall. After obtaining parasternal long-axis view (Figure 10), the transducer was rotated 90° clockwise and angulated until the desired images of short axis view were obtained. LV internal dimensions were measured through the largest diameter of the ventricle, both in diastole and systole. FS was calculated according to the following formula:

$$FS = (LVDD - LVDs) / LVDD \times 100\%$$

where LVDD is the left ventricular diameter in diastole, and LVDs is the left ventricular diameter in systole (Fig. 12).

2.4.2 Doppler Measurements

Pulsed wave Doppler spectra of mitral inflow were recorded from the apical four-chamber view (Fig. 13, 14). The four-chamber view which shows the mitral and tricuspid valves simultaneously was obtained by placing the transducer in the cardiac apex and angling anteriorly. The sample volume (0,5mm - the smallest available size) was placed at the tip of the mitral leaflets and adjusted to the position at which velocity was maximal. All echocardiographic measurements were conducted in accordance with the recommendation of the American Society of Echocardiography.



Figure 9: A high-resolution imaging echocardiography system Vevo 770 (VisualSonics Inc., Toronto) equipped with a 25 MHz single-crystal transducer.

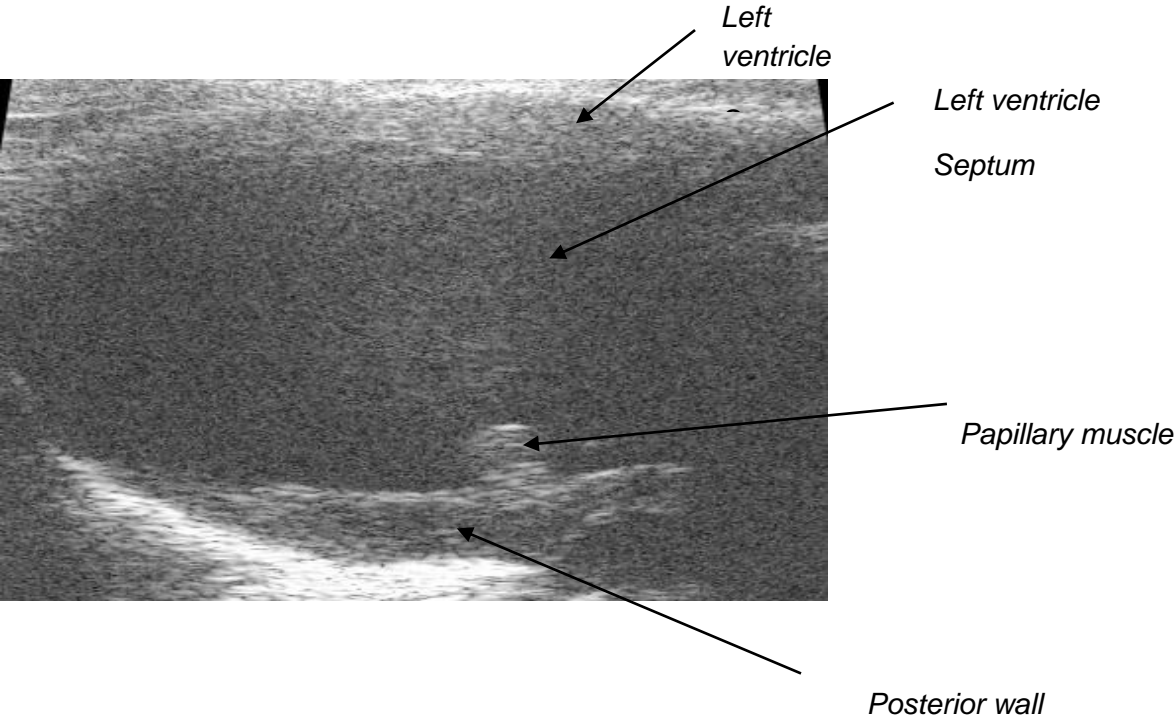


Figure 10: 2D Pictures. Parasternal long axis view: left ventricle.

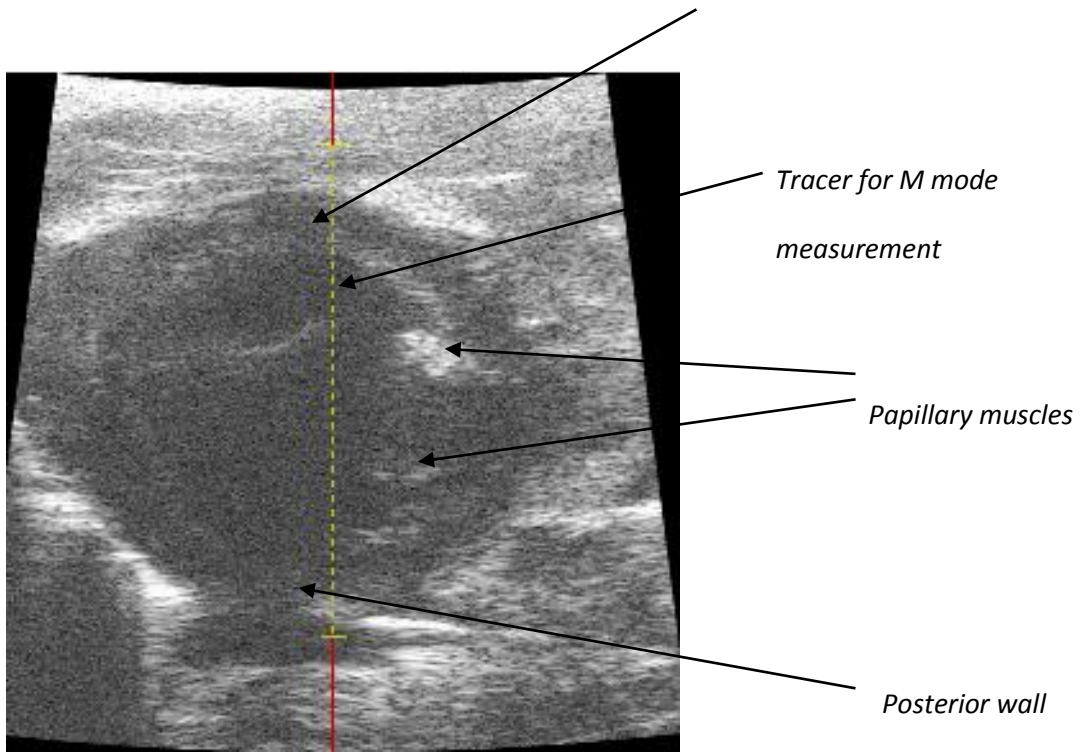


Figure 11: Parasternal short axis view (2D): left ventricle.

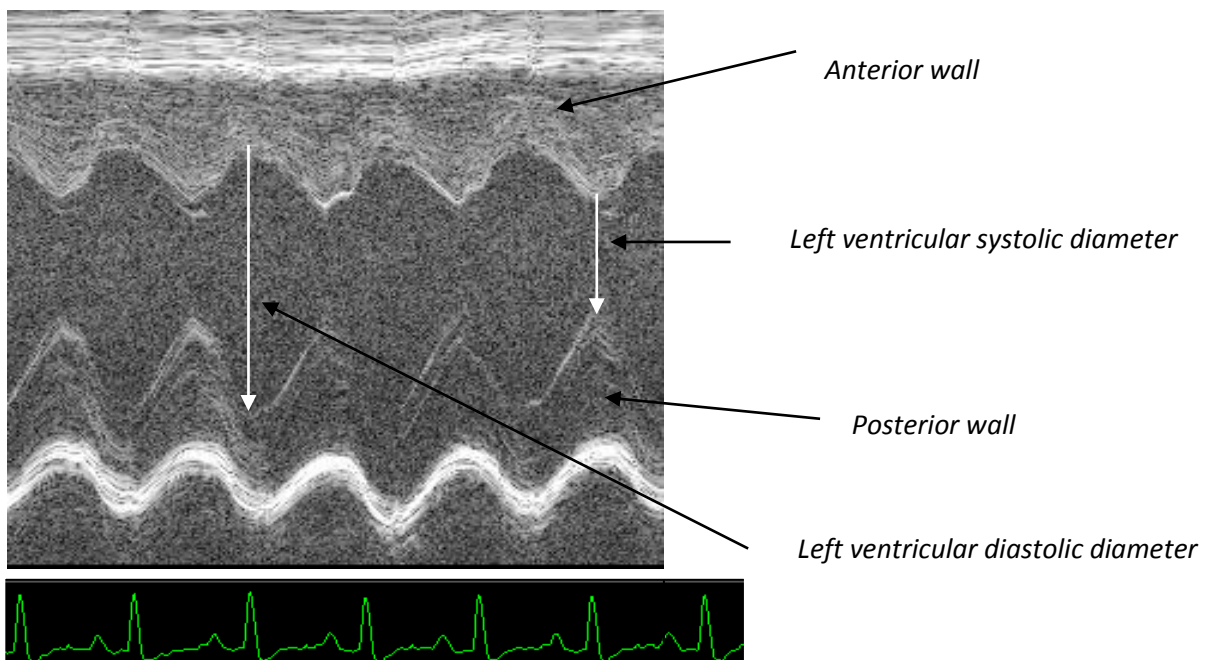


Figure 12: M mode from short axis view.

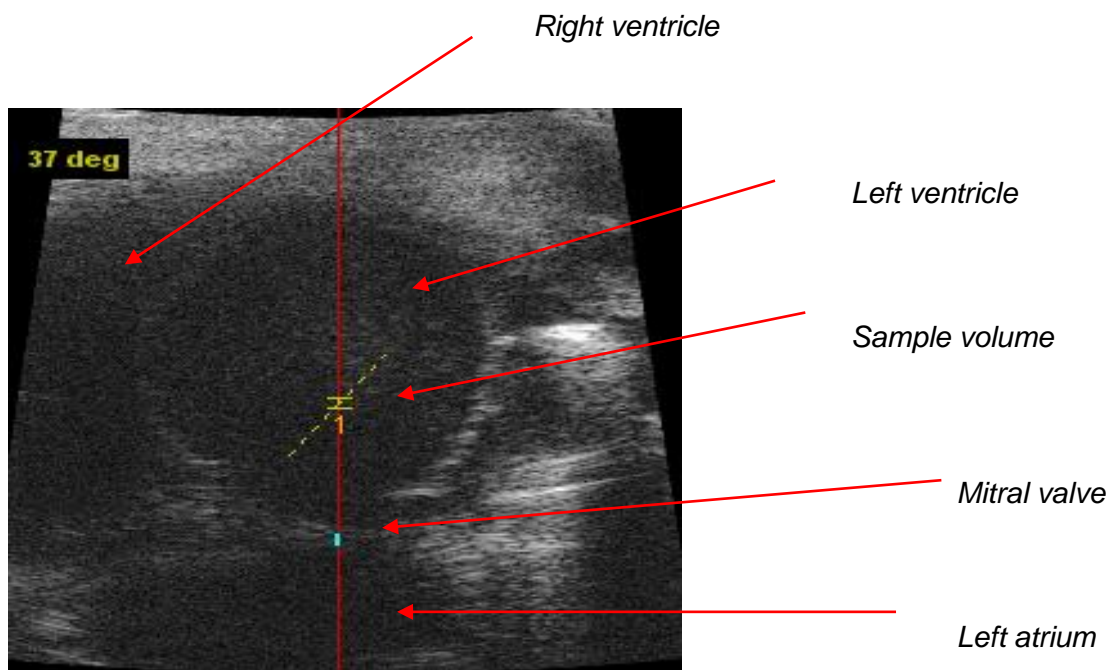


Figure 13: Four chamber view (2D).

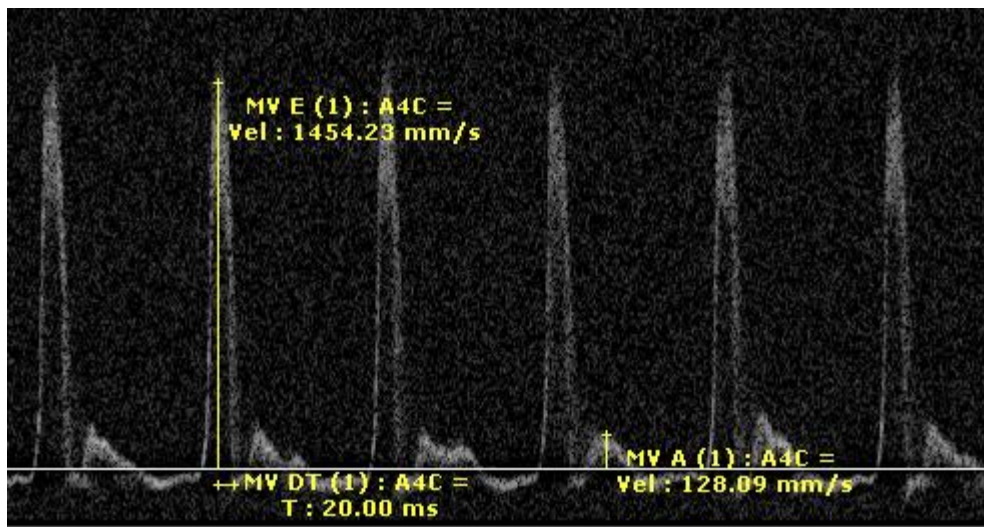


Figure 14: Doppler spectra of mitral inflow obtained from 4 chamber view.

2.5 Determination of Left Ventricular and Scar Volumes by Magnetic Resonance Imaging

This method was performed in cooperation with the German Heart Center in Berlin.

Cardiovascular MRI has a high spatial resolution and moderate temporal resolution. It is a well-validated standard for the assessment of myocardial function. Cardiac-triggered cine and scar magnetic resonance imaging was performed on a conventional clinical 3.0 Tesla scanner (Philips Achieva CV 3.0T, Best, The Netherlands) equipped with a QuasarDual gradient system (80mT/m; 200mT/m/ms slew rate) using specifically designed software (release 2.5.1 with implementation of a small animal software patch developed by GyroTools Ltd., Zurich, Switzerland). All animals were examined in the supine position and placed in a solenoid radiofrequency coil used for signal detection. Cardiac synchronization was performed using four electrodes (vector-electrocardiogram) fixed to the anterior chest wall and scans were triggered on the R-wave of the electrocardiogram. The animals were anesthetized by inhalation of isoflurane via a nose cone at a 1.0%–1.5% volume mixed with oxygen at a rate of 2 liter/min.

For cine imaging, a gradient echo pulse sequence (TR/TE/flip angle/number of signal averages = 9.0 msec/4.2 msec/15°/5) was used for complete coverage of the heart in short axis geometry (spatial resolution 0.2 x 0.2 mm, slice thickness 1.5 mm, number of slices 9) with 30 phases/cardiac cycle acquired per slice (Fig. 15).

Scar imaging was started 2 min after tail injection of gadolinium-DTPA (0.2 mmol/kg bodyweight) employing a 3-dimensional inversion-recovery sequence (TR/TE/flip angle/number of signal averages = 6.7 msec/3.3 msec/15°/2) with an individually adapted inversion prepulse delay (range 100 to 130 ms). In-plane spatial resolution of scar imaging was 0.15 x 0.15 mm with a slice thickness of 0.8 mm (Fig. 16).

All scans were processed with dedicated image analysis software (Philips View Forum, release 5.1.1.1, Best, The Netherlands). For left ventricular volume measurements, the endocardial border of each short axis slice was planimeted manually at end diastole and end systole, and volumes were calculated by using the Simpson rule. End diastole was defined as the first frame in each cine sequence and end systole as the cine frame with the smallest left ventricular cavity area. For determination of scar volume, the brightly enhanced scar area was manually segmented in each slice and multiplied with slice thickness for calculation of scar volume.

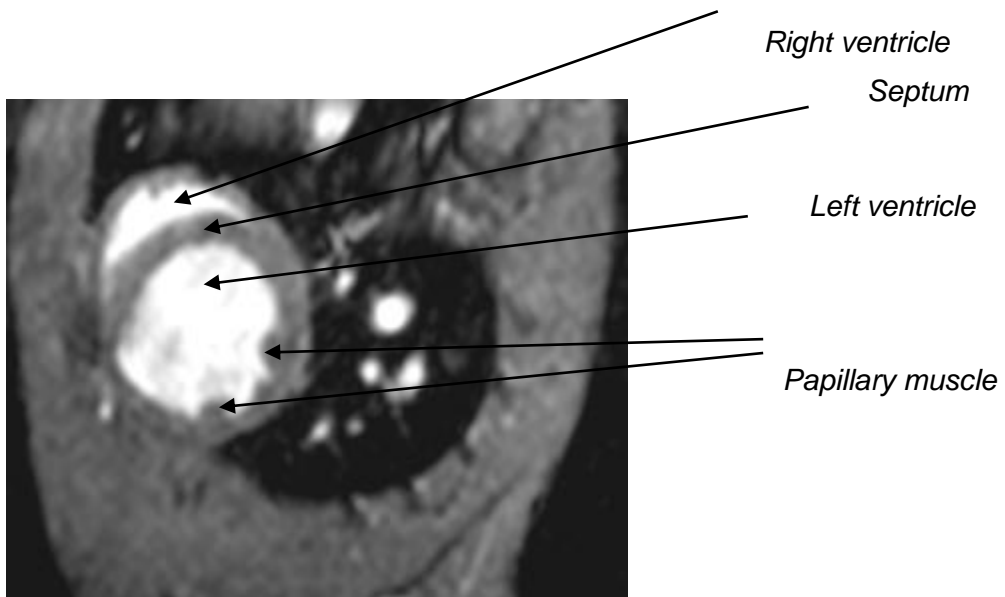


Figure 15: Short axis view of the heart in diastole.

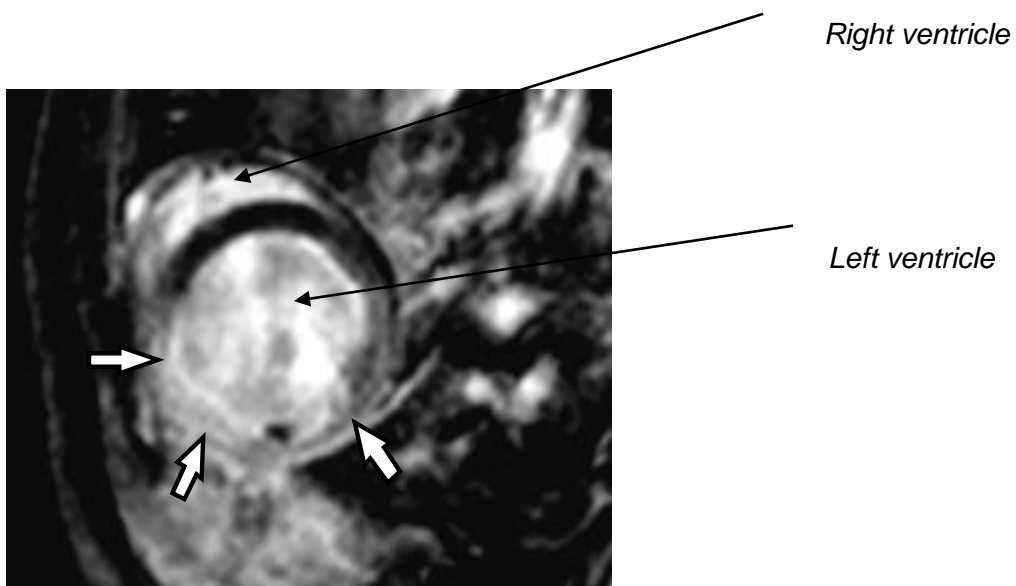


Figure 16: Infarcted wall of the left ventricle after gadolinium-DTPA enhancement.

2.6 Millar catheter

On day 7 after MI, prior to sacrifice, rats were anesthetized with ketamin/xylazine (80 mg/10 mg/kg i.p). A SPR-407 MikroTip pressure catheter transducer (Millar Instruments, Houston, USA) was passed through the right carotid artery and inserted into the aorta for recording the heart rate and arterial pressure under constant pressure monitoring (Fig. 17). The catheter was then advanced into the left ventricle (LV) for measurement of cardiac parameters. The catheter was connected via PowerLab/4 unit (ADInstruments) to a computer running MacLab (Chart 5 software). Data were recorded over 10min, stored and later analyzed with Chart software (Blood Pressure Module), (Fig. 18).

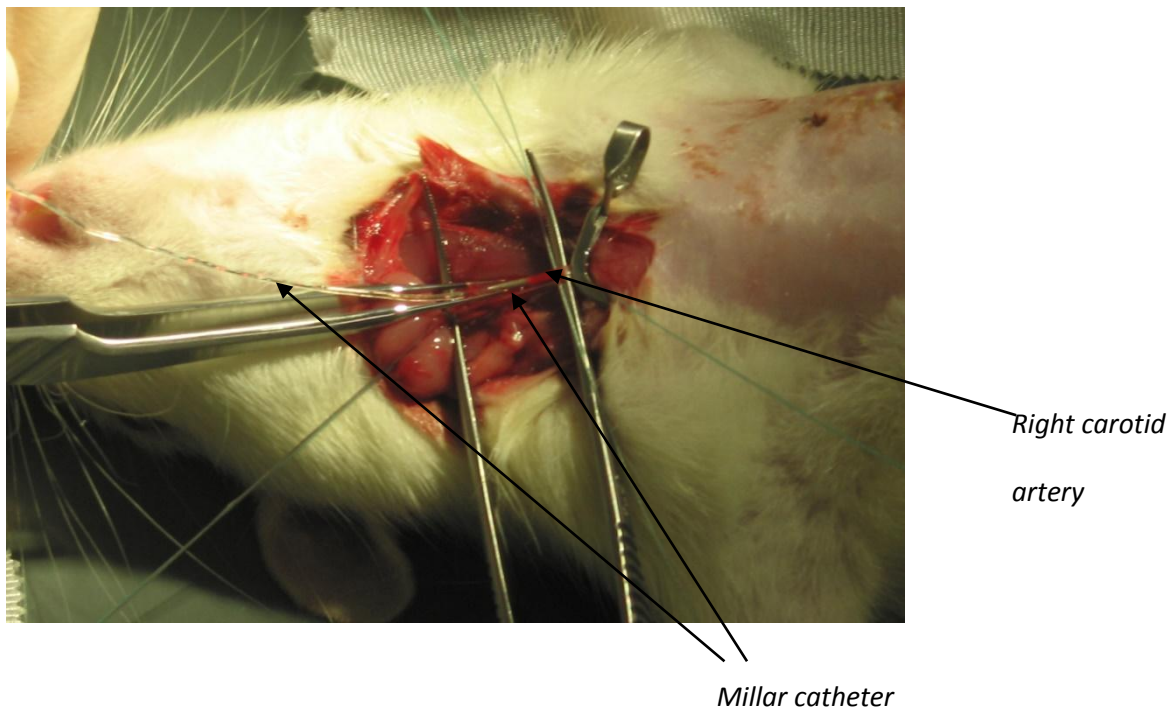
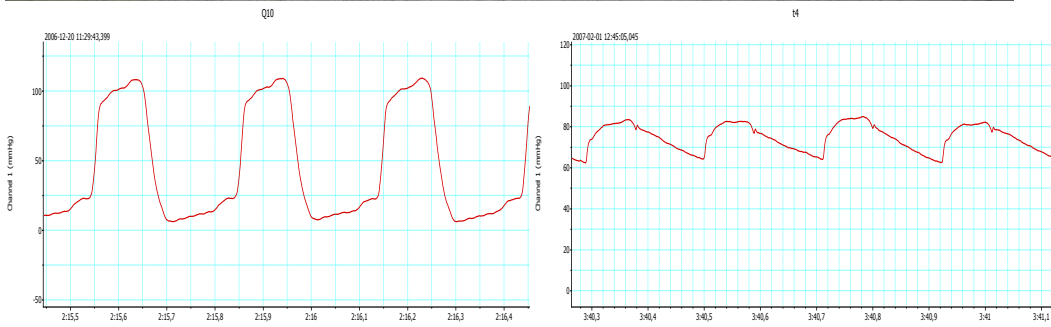
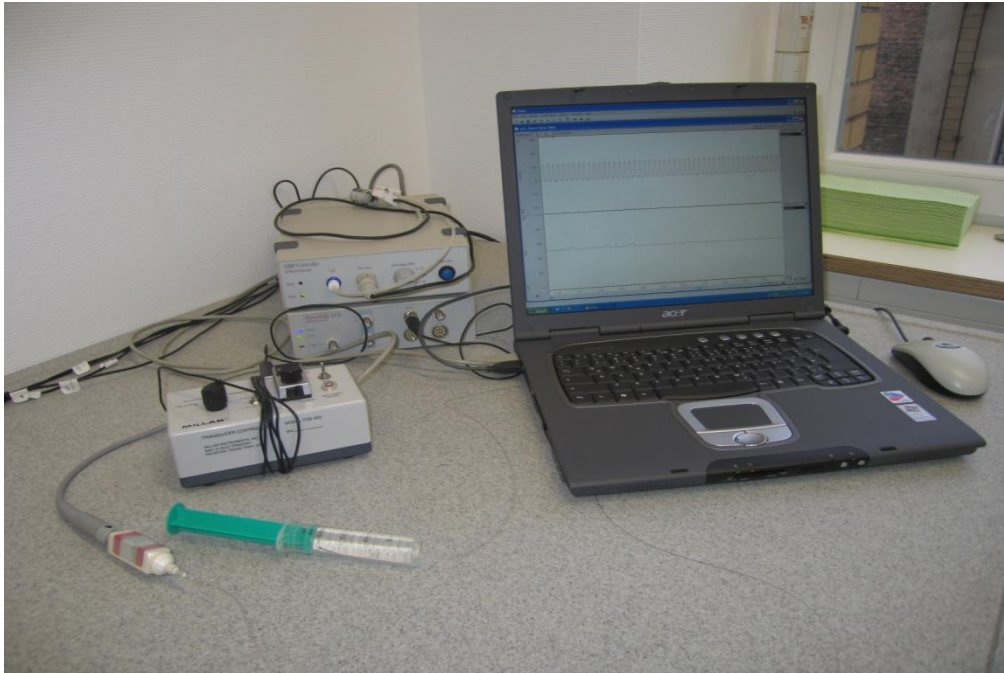


Figure 17: Surgical placement of Millar catheter in carotid artery.



A.

B.

Figure 18: PowerLab/4 unit with connected Millar catheter. A: Left ventricle pressure curve. B: Aorta pressure curve.

2.7 Plasma Monocyte-chemoattractant Protein-1 (MCP-1) and Myelo-peroxidase (MPO) ELISAs

Plasma MCP-1 (Biosource International) and MPO (Immundiagnostic AG, Bensheim, Germany) levels were determined by commercially available ELISA kits according to the manufacturer's instructions.

In brief, plasma samples for the detection of MCP-1 were diluted in standard diluent, and 50 μ l samples were added to each well of an anti-Rat MCP-1 pre-coated 96-well strip plate followed by an one hour incubation at room temperature. Samples were then incubated for another hour with a biotinylated antibody reagent. After adding streptavidin, absorbance was measured on an ELISA plate reader (Bio-Rad, Benchmark Plus) at 450 nm against 550 nm. Plasma amounts of MCP-1 were calculated referring to a standard curve.

For the detection of MPO, diluted plasma samples were incubated for one hour in an anti-rat MPO pre-coated 96 well microtiter plate, and for an additional hour with a peroxidase-coupled antibody. Absorbance was measured at 550 nm against 620 nm as a reference, and plasma amounts of MPO calculated referring to a standard curve.

2.8 Quantitative real-time RT-PCR (qPCR)

Total RNA was isolated from cardiac tissue (peri-infarct zone) using Trizol reagent (Invitrogen) according to the manufacturer's protocol. RNA (1 μ g) was reverse transcribed in 25 μ l final volume for 1 hour at 37 °C using 100 U Superscript Reverse Transcriptase, 5.0 μ g random primer, 0.5 mM 2'-deoxynucleotide5' triphosphate, 20 U RNAsin, and 5 μ l 5x reaction buffer. Relative quantification of gene expression was performed with the ABI 5700 sequence detection system for real-time polymerase chain reaction (PCR; TaqMan technology by PE Biosystems, Weiterstadt, Germany) using the standard curve method. PCRs were performed with the TaqMan Universal Master Mix and the TaqMan assay reagent for GAPDH in a total volume of 25 μ l.

Each qPCR reaction was performed in triplicate wells, using the following conditions: activation of Taq-Polymerase 5 min at 95°C, 15 s at 95°C, 15 s at 60°C, 30 s at 72°C through 40 cycles, followed by 15 s at 50°C.

Data represent the mean expression level \pm standard deviation (standardized to beta-actin mRNA expression) calculated according to the ddCT method of at least three independent measurements.

2.9 Western Blot Analysis

Tissue samples were homogenised in lysis buffer (50 mM Tris-HCl, 500 mM EDTA, 150 mM NaCl, 0.1% Triton X-100) supplemented with 100 µg/ml PMSF and protease-inhibitor-cocktail (Roche) followed by centrifugation. Protein concentrations were determined by the Bradford method using BSA as a standard. Proteins (30µg per line) were separated by 10% SDS-PAGE and transferred to nitrocellulose membranes (Amersham). Membranes were blocked in 5% non-fat milk/TTBS, and incubated consecutively with primary antibody and horseradish peroxidase-conjugated secondary antibody (Dako). Immunoreactive proteins were detected using ECL-reagents (Amersham). The following primary antibodies were used: FasL (1:500; Cell Signaling Technology Inc.), caspase 3 (1:500; Cell Signaling Technology Inc.), phospho-p44/42 MAPK, phospho-p38 MAPK (Phospho-MAPK Family Antibody Sampler Kit, Cell Signaling Technology Inc., USA), p44/42 MAPK, and p38 MAPK (MAPK family Antibody Sampler, Cell Signaling Technology Inc., USA). Computer assisted Quantification of Western Blots was performed using the NIH image analysis system (Scion, Frederick, MD, USA). To demonstrate equal protein loading of the gel, membranes were reprobbed with GAPDH Ab (Acris).

Materials

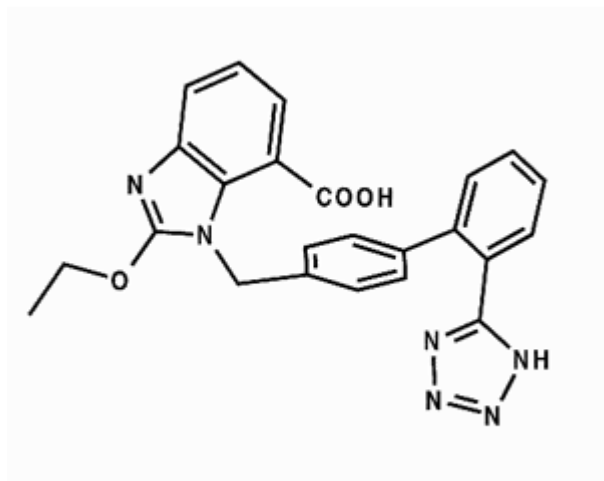
3.1 Substances and Chemicals

Acrylamid	Roth, Karlsruhe, D
Agarose	QA-Agarose™, Q-BIOgene, USA
Ammoniumpersulfat (APS)	Sigma, Taufkirchen, D
Bovines Serumalbumin (BSA)	Sigma, Taufkirchen, D
Bromphenolblau	Sigma, Taufkirchen, D
Electrode gel- Spectra 360	Parker Laboratories INC, USA
Ethanol 70%, 90%, 96%, 100%	Merck KGaA, Darmstadt, D
Glycin	Sigma, Taufkirchen, D
LB-Agar,	Becton Dickenson, Sparks, USA
LB-Broth, Miller	Becton Dickenson, Sparks, USA
N,N,N',N'-Tetramethylethyldiamin (TEMED)	Sigma, Taufkirchen, D
NaCl	Merck KGaA, Darmstadt, D
NP40 10% (v/v)	Sigma, Taufkirchen, D
10x PCR-Puffer und MgCl ₂ (25 mM)	Promega GmbH, Mannheim, D
5x M-MLV-Puffer	Promega GmbH, Mannheim, D
Paraffin Typ 9	Microm GmbH, Walldorf, D
Ponceau-S	Sigma, Taufkirchen, D
Proteaseinhibitoren Complete-Mini	Roche Diagnostics, Mannheim, D
Restore™ Western stripping buffer	Pierce
Sodium-Nitroprussid	Sigma, Taufkirchen, D
TEMED	Sigma, Taufkirchen, D
Trizma-Base	Sigma, Taufkirchen, D
Trizol	Invitrogen, Karlsruhe, D
Tween 20	Sigma, Taufkirchen, D
Ultrasound gel- Aquasonic clear	Parker Laboratories INC, USA
Xylol	Merck KGaA, Darmstadt, D

3.1.1 Drugs

Candesartan

Structural formula:



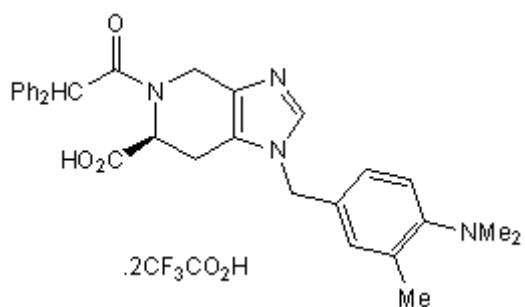
Empirical formula: C₂₄H₂₀N₆O₃

Molecular weight: 440.454 g/mol

Function: AT1 receptor blocker

PD 123

Structural formula:



Empirical formula: C₃₁H₃₂N₄O₃·2CF₃CO₂H

Molecular weight: 736.67 g/mol

Function: AT2 receptor antagonist.

3.2 Kits

BCA™ Protein Assay Reagent Kit	Perbio Science, Piece, Bonn, D
ECL Western Blotting Detection Reagents	Amersham-Pharmacia, Freiburg, D
NucleoSpin Plasmid Quick Pure	Macherey-Nagel, Düren, D
ProteoExtract™ Subcellular ProteomeExtractionKit	Calbiochem, Schwalbach, D

Real-time PCR-Mastermix:

Components	Preparation	µl per 25 µl reaction volume
H ₂ O		10,225
	100 mM Tris HCl	
	15 mM MgCl ₂	
10x PCR-Puffer	500 mM KCl (pH 8,3)	2,5
MgCl ₂	50 mM	2,5
dNTPs	10 mM pro Nukleotid	0,5
	20% DMSO in H ₂ O mit 10x SYBR	
SYBR Green	(1:1000 Dilution)	2,5
	0,5% NP40 (v/v)	
NP40/ Tween 20	0,5% Tween 20 (v/v)	0,25
	One crystall ROX in ca. 50 ml H ₂ O	
ROX	solution.	0,25
Taq-Polymerase	5 U/µl	0,075
forward Primer	10 µM	0,6
reverse Primer	10 µM	0,6
cDNA		10
Total volume		30

3.3 Electrophoresis and Blot System

Vertikal Elektrophorese-Systeme, Midi und Maxi
Horizon™58 Bethesda Research Laboratories,
Horizontal Elektrophorese-Systeme, Mini-Protean®
Semi-Dry Blot-System

Harnischmacher, Kassel, D
Gaithersburg, USA
Bio-Rad, München, D
Bio-Rad, München, D

3.4 Centrifuges and Rotors

Table centrifuge Mikro 20, Typ2004
Galaxy Mini
Centrifuge 5415R
Centrifuge Mikro 22R
Centrifuge 5402
Vortex 3005

Hettich, Zentrifugen, Tuttlingen, D
Merck KGaA, Darmstadt, D
Eppendorf, Hamburg, D
Hettich Zentrifugen, Tuttlingen, D
Eppendorf®, Hamburg, Deutschland
G.F.L®, Burgwedel, Deutschland

3.5 Microscope

Light-microscope Leica DMIL

Leica, Wetzlar GmbH, Deutschland

3.6 Operation Equipment

Diverse operating equipment

Suture:

Prolene 17mm (polypropylen) not absorbable
Ethibond excel 13mm (polyester) not absorbable
Ethibond excel 3.5 Ph (polyester)
Terylene USP 4/0
Syringe BD
Microlance 3 BD
Echocardiography-VisualSonics Vevo 770
Millar catheter SPR-407

Ethicon
Ethicon
Ethicon
Serag Wiessner, Germany
Franklin Lakes USA
Becton Dickintion Spain
Toronto Ontario, Canada
Millar Instruments, Houston, USA

3.7 Buffers

3.7.1 Protein extraction

Protein lysis buffer: 20 mM Tris-Base (pH 7,5)
 150 mM NaCl
 1 mM EDTA
 1 mM EGTA
 2,5 mM 1% Triton-X 100
 2,5 mM Natriumpyrophosphat
 1 mM Natriumorthovanadat
 1 Tablette Proteaseinhibitoren Complete Mini per 10 mL

3.7.2 Western Blot Buffers

1x Elektrophoresis buffer: 3 g Tris-Base
 14,4 g Glycin
 1 g SDS
 add 1 L H₂O

Semi-Dry Blott buffer: 5,82 g Tris-Base
 2,93 g Glycin
 200 mL Methanol
 0,375 g SDS
 ad 1 L H₂O
 pH 9,0 – 9,4

10x Tris-buffered saline (TBS): 60,57 g Tris-Base
 43,83 g NaCl
 add 500 mL H₂O
 pH 7,5

1x TBS-T: 100 mL 10x TBS
 1 mL Tween 20
 add 1 L H₂O

Results

4.1 Basal Parameters

Postinfarct mortality amounted to 31%. Animal losses all occurred within the first 24 hours after MI, in which animals were not yet treated, and were equally distributed among future treatment groups. No animals died on day 2 to 7 after MI.

Body and heart weight did not differ between treatment groups or between animals with or without myocardial infarction (data not shown).

4.2 Magnetic Resonance Imaging

Magnetic resonance imaging was performed at day 7 after MI or sham operation. The following groups were scanned: MI / vehicle; MI / candesartan; MI / C21; MI / candesartan /C21. MRI revealed that only C21 significantly reduced scar volume which is related to extend of MI ($14.6 \pm 1.4\%$, $p < 0.05$) compared to vehicle ($20.5 \pm 2.2\%$). In candesartan- treated group this effect was not observed ($20.7 \pm 1.4\%$). Also the combination therapy C21/candesartan did not significantly reduced scar volume ($18.4 \pm 2.3\%$), (Table 1, Fig.18). Furthermore, ejection fraction was significantly improved in C21 (EF $54.4 \pm 1.9\%$, $p < 0.0005$), C21/candesartan (EF $51.3 \pm 3\%$, $p < 0.0005$) and, to a lesser extent, candesartan- treated group (EF $42.6 \pm 3\%$, $p < 0.05$), compared to vehicle (EF $31.7 \pm 2.1\%$) (Table 1).

Table 1: Magnetic Resonance Tomography 7 Days after MI.

	Sham	Myocardial infarction			
		Vehicle	Comp 21 0.03 mg/kg	Candesartan 0.1 mg/kg	Comp21+Cand
EF(%)	66.7±0.4	31.7±2.1*	54.4±1.9*¥	42.6±3 [#]	51.3±3*¥
Scar Volume(%)		20,5±1.5	14,6±1.4 [#]	20.7±1.4	18.4±2.3

* $p < 0.0001$ vs sham; [#] $p < 0.05$ vs vehicle; ¥ $p < 0.0005$ vs vehicle.

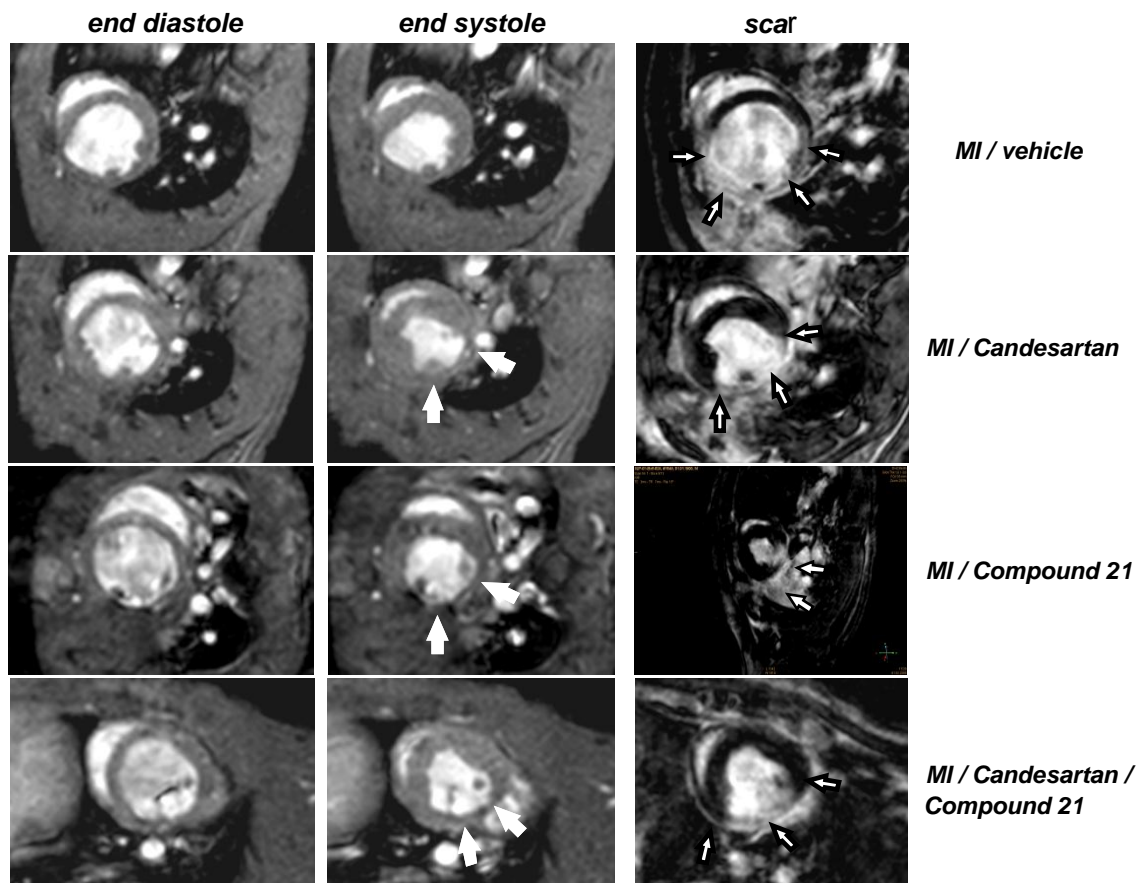


Figure 18: Representative cine MR images (left, enddiastolic frame; right: endsystolic frame) and corresponding delayed enhancement MR imaging. White arrows: segmental wall motion abnormalities; black-rimmed white arrows: segmental extent of scar tissue (i.e. brightly signal- enhanced myocardium on post-contrast images with non-scarred myocardium appearing black).

4.3 Hemodynamic Measurements (Millar catheter)

Hemodynamic parameters obtained on day 7 after MI or sham operation by Millar catheter in animals with minor to moderate post-infarct impairment of cardiac function (EF >35%) are presented in Table 2 and Fig. 19, those obtained in animals with severe impairment of cardiac function (EF <35%) in Table 5 at the end of this chapter.

Millar catheter

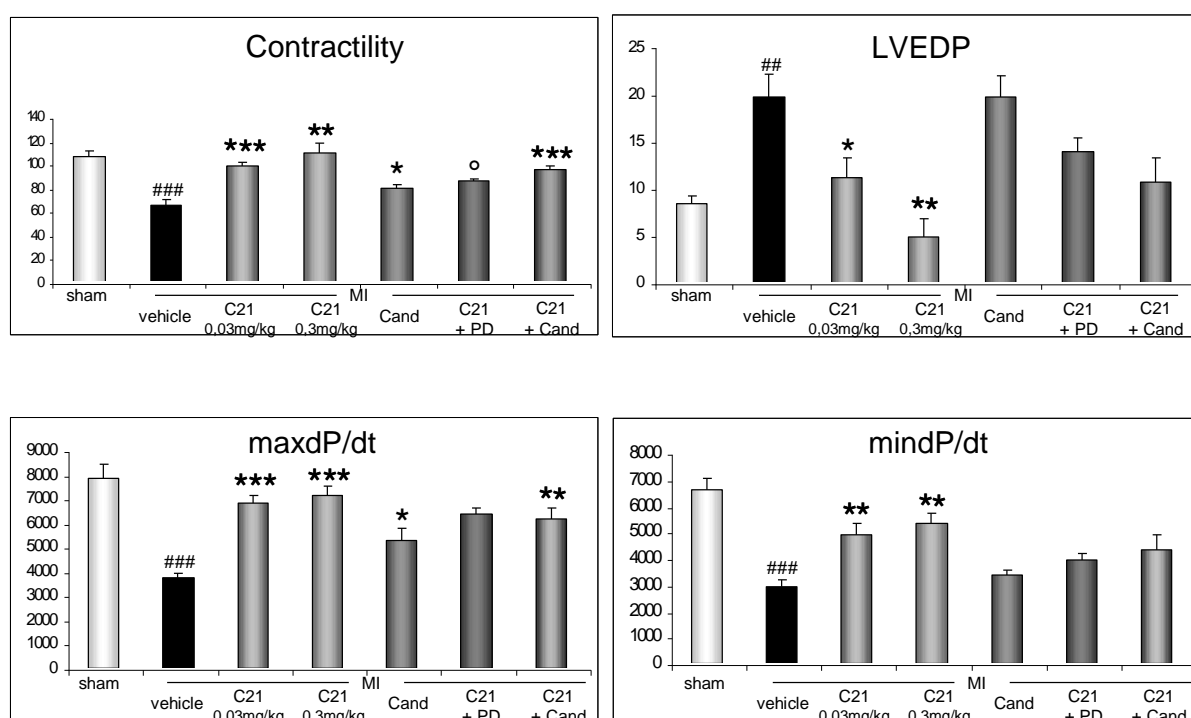


Figure 19: Hemodynamic parameters measured by Millar catheter.

p < 0.005 vs sham; ## p < 0.005 vs sham; *** p < 0.0005 vs vehicle; ** p < 0.005 vs vehicle; * p < 0.05 vs vehicle; ° p < 0.05 vs C21. LVEDP- left ventricle end diastolic pressure, maxdP/dt: max peak rate of LV-pressure, mindP/dt: min peak rate of LV- pressure.

Rats with MI had significant systolic dysfunction, as evidenced by a significant decrease in contractility (67 ± 2.9 1/s, $p < 0.005$ compare to sham 106 ± 2.7 1/s) and in maximal peak rate (maxdP/dt) of left ventricular pressure (3664 ± 114 mmHg/s, $p < 0.005$, compared to sham 7532 ± 321 mmHg/s). Rats with MI also had severe diastolic dysfunction, as defined by a significant elevation of LV end-diastolic pressure (22.9 ± 1.5 mmHg, $p < 0.005$, compared to sham 7.5 ± 0.6 mmHg) and a significant decrease in minimal peak rate (mindP/dt) of left ventricular pressure (2967 ± 191 mmHg/s, $p < 0.005$, compared to sham 6795 ± 231 mmHg/s), (Table 2, Fig. 19).

LV end-diastolic pressure was significantly reduced only in C21 (0.03mg/kg) (13 ± 1.6 mmHg, $p < 0.005$), C21(0.3mg/kg) (9 ± 1.3 mmHg, $p < 0.005$) and C21/candesartan treated group (12.4 ± 1.7 mmHg, $p < 0.05$) compared to vehicle (22.9 ± 1.5 mmHg).

Contractility was significantly improved in C21 (0.03mg/kg) (96 ± 2.5 1/s, $p < 0.0005$), C21 (0.3mg/kg) (97 ± 3.8 1/s, $p < 0.0005$), C21/candesartan (95.2 ± 3.4 1/s, $p < 0.0005$) and, to a lesser extent, in candesartan treated group (81 ± 2.3 1/s, $p < 0.005$) compared to vehicle (67 ± 2.9 1/s).

Maximal peak rate (maxdP/dt) of left ventricular pressure was significantly enhanced in C21 (0.03mg/kg) (6667 ± 235 mmHg/s, $p < 0.0005$), C21 (0.3mg/kg) (6950 ± 261 mmHg/s, $p < 0.0005$), C21/candesartan (6280 ± 319 mmHg/s, $p < 0.005$) and, to a lesser extent, in candesartan treated group (5193 ± 278 mmHg/s, $p < 0.05$) compared to vehicle (3664 ± 114 mmHg/s).

Minimal (mindP/dt) peak rate of left ventricular pressure was significantly enhanced in C21 (0.03mg/kg) (5129 ± 277 mmHg/s, $p < 0.0005$), C21 (0.3mg/kg) (5198 ± 309 mmHg/s, $p < 0.0005$), and, to a lesser extent, in C21/candesartan treated group (4805 ± 315 mmHg/s, $p < 0.005$) compared to vehicle (2967 ± 191 mmHg/s). This effect was not observed in candesartan treated group (3385 ± 163 mmHg/s).

The AT2R antagonist, PD 123319, significantly abolished the effects of C21 on contractility (83 ± 1.5 1/s, $p < 0.05$ vs C21 97 ± 3.8 1/s), partly on mindP/dt (3861 ± 214 mmHg/s vs C21 5198 ± 309 mmHg/s) and LVEDP (15.7 ± 1 mmHg vs C21 9 ± 1.3 mmHg), (Table 2, Fig.19). A combination of C21 and candesartan was not more effective than C21 mono-therapy.

In animals with severe post-infarct impairment of cardiac function (EF < 35%), C21 (0.03 mg/kg) still led to a significant improvement of LVEDP (11.6±2.6 mmHg, p<0.005 vs vehicle 23.9±1.4 mmHg), contractility (92±4 1/s, p<0.005 vs vehicle 58±8 1/s) and maxdP/dt (5997±641 mmHg/s, p<0.05 vs vehicle 3730±476 mmHg/s), and tended to improve mindP/dt (4088± 599 mmHg/s vs vehicle 3200± 693 mmHg/s), (Table 5). There was a significant improvement of cardiac function in animals treated with 0.03 mg/kg which was only slightly and not in all cases further improved in animals treated with 0.3 mg/kg (Fig. 19, Table 2).

Table 2. Hemodynamic Parameters Measured by Millar Catheter 7 Days After MI

	MI						
	Sham n=12	Vehicle n=12	Comp21 0.03mg/kg n=12	Comp21 0.3mg/kg n=12	Candesartan 0.1mg/kg n=12	Comp21+PD n=12	Comp21+Cand n=12
VSP[mmHg]	129±5	115±3	124±4	112±5	115±6	117±7	112±5
LVEDP[mmHg]	7.5±0.6	22.9±1.5 ^{###}	13±1.6 ^{**}	9.0±1.3 ^{**}	18.8±1.7 ^{##}	15.7±1.0 [#]	12.4 ±1.7 [*]
Contractility Index[1/s]	106±2.7	67±2.9 ^{###}	96±2.5 ^{***}	97±3.8 ^{***}	81±2.3 ^{###}	83±1.5 ^{##o}	95.2±3.4 ^{***}
maxdP/dt[mmHg/s]	7532±321	3664±114 ^{###}	6667±235 ^{***}	6950±261 ^{***}	5193±278 [#]	4964±214 [#]	6280±319 ^{#**}
mindP/dt[mmHg/s]	6795±231	2967±191 ^{###}	5129±277 ^{###}	5198±309 ^{***}	3385±163 ^{###}	3861±214 ^{##}	4805±315 ^{###}
SBP[mmHg]	122±6	115±3	124±6	115±5	115±7	117±4	114±6
DBP[mmHg]	86±2	83±3	86±3	81±4	80±6	84±3	84±5
Pulse Pressure[mmHg]	35±2	32±2	37±3	34±3	35±2	33±3	30±3
HR[bpm]	239±5	258±19	232±10	248±6	252±10	240±9	246±10

VSP: ventricular systolic pressure, LVEDP: left ventricular end diastolic pressure, maxdP/dt: max peak rate of LV-pressure, mindP/dt: min peak rate of LV-pressure, SBP: systolic blood pressure, DBP: diastolic blood pressure, HR: heart rate

^{###}p<0.005 vs Sham; ^{##}p<0.005 vs Sham; [#]p<0.05 vs Sham; ^{***}p<0.0005 vs vehicle; ^{**}p<0.005 vs vehicle; ^{*}p<0.05 vs vehicle; ^op<0.05 vs Comp.21

4.4 Transthoracic Doppler Echocardiography

Transthoracic echocardiography was performed 1 day after MI/sham operation to estimate EF before starting the treatment. There were no significant differences in EF between the groups (Fig. 20).

Transthoracic Echocardiography was performed again 7 days after MI or sham operation to obtain systolic and diastolic function of the heart.

There were no changes in heart rate between the groups (Table 3).

Myocardial infarction caused a significant impairment of systolic and diastolic heart function. After MI, there was a significant increase in systolic (6.3 ± 0.2 mm, $p < 0.0001$ vs sham 3.8 ± 0.11 mm) and diastolic (8.7 ± 0.2 mm, $p < 0.0001$ vs sham 7.1 ± 0.14 mm) left ventricular inner diameter (LVIDs; LVIDd).

Ejection fraction (EF) and fractional shortening (FS) after MI significantly decreased (EF 49 ± 2 %, $p < 0.0001$ vs sham 77 ± 1.1 %), (FS 26.1 ± 1.6 %, $p < 0.0001$ vs sham 46.3 ± 1.2 %), (Table 3).

Examples of freeze-frame M mode echocardiographic short-axis images from a sham-operated rat and a rat with MI are shown in Fig. 21 A.

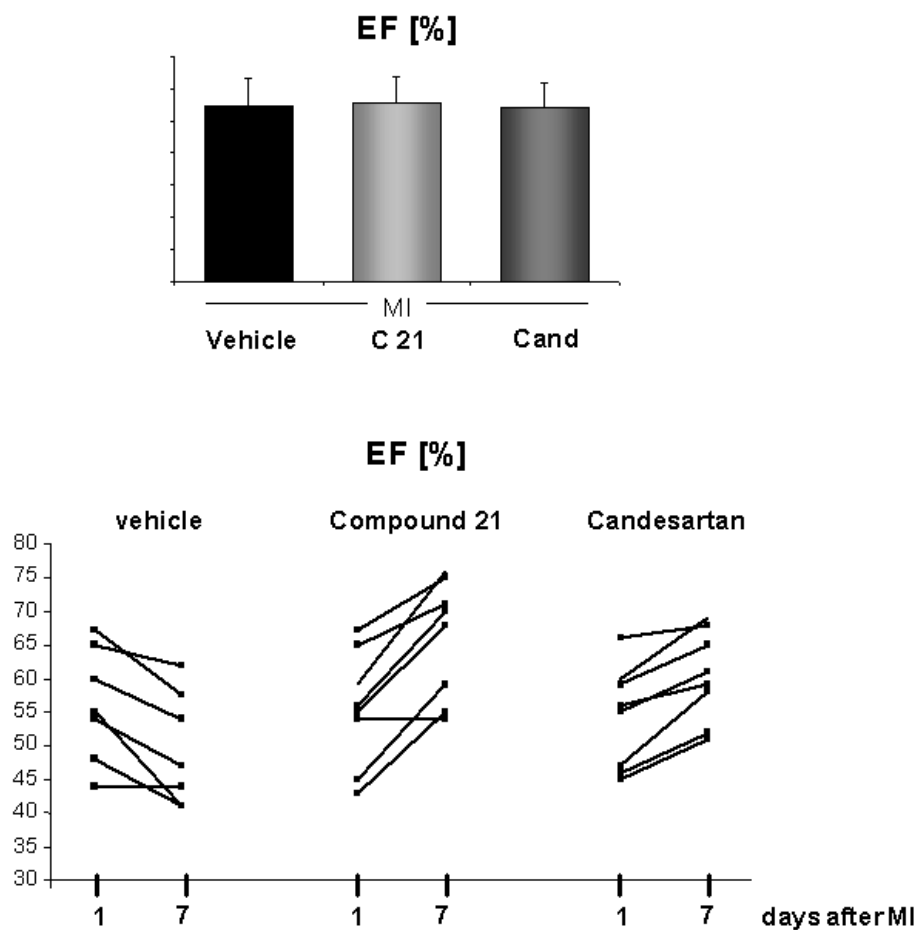


Figure 20: EF 1 day after MI measured by echocardiography. (A) EF measured 1 day after MI before starting treatment. No significant differences between the groups were observed. (B) Change of ejection fraction in individual animals with EF>35 from treatment start (day 1) to the end of treatment (day 7).

Table 3. Transthoracic Doppler Echocardiography Measurements 7 Days After MI

	MI						
	Sham	Vehicle	Comp21 0.03mg/kg	Comp21 0.3mg/kg	Candesartan 0.1mg/kg	Comp21+PD	Comp21+Cand
LVIDd,mm	6.9±0.16	8.1±0.1 ^{###}	7.3±0.12 ^{***}	7.5±0.13 ^{**}	7.7±0.1 ^{##} *	8±0.4 [#]	7.6±0.17 [#]
LVIDs,mm	3.7±0.14	5.9±0.2 ^{###}	4.3±0.2 ^{***}	4.9±0.2 [#] *	5±0.2 ^{###} *	6.13±0.5 ^{###00}	4.9±0.3 ^{##} **
FS,%	45.5±1.4	27.5±2.2 ^{###}	40.4±2.5 ^{**}	34.7±2 ^{###} *	36.5±2 ^{##} *	22.4±1.9 ^{###00}	35.4±2 ^{##}
EF,%	76±1.3	51±3.0 ^{###}	69±3 ^{**}	62±2.7 ^{###} *	61±3 ^{###} *	43±3.5 ^{###000}	62.5±3.6 ^{##}
E,mm/s	1105±36	1517±26 ^{###}	1138±20 ^{***}	1096±36 [*]	1176±59 ^{***}	1378±41 ^{##00}	1312±68 ^{##} **
A,mm/s	648±40	241±22 ^{###}	513±36 ^{***}	504±54 [*]	602±77 ^{**}	222±41 ^{###00}	631±75 ^{***}
E/A	1.7±0.07	6.5±0.58 ^{###}	2±1.3 ^{***}	1.9±0.06 ^{***}	1.7±0.08 ^{***}	6.7±1.14 ^{###00}	2.2±0.2 ^{***}
EDT,ms	26.4±0.6	14±1 ^{###}	22±1 ^{**}	20±0.5 ^{**}	21±1.5 ^{**}	16±0.5 ⁰⁰⁰	20±0.9 ^{###} **
HR	369±15	391±13	376±10	369±16	374±6	402±16	384±11

LVIDd:left ventricular internal dimension end diastole, LVIDs:left ventricular internal dimension end systole, FS:fractional shortening, EF:ejection fraction, E:peak velocity of early filling wave, A:peak velocity of late filling wave, EDT:E wave deceleration time, HR: heart rate. [#]p<0.05 vs sham ^{###}p<0.0001 vs sham; ^{***}p<0.0001 vs vehicle; ^{**}p<0.001 vs vehicle; ^{*}p<0.05 vs vehicle; ⁰⁰⁰p<0.0001 vs Comp21; ⁰⁰p<0.001 vs Comp21; ⁰p<0.05 vs Comp21

MI caused profound alterations of LV diastolic filling characterized by significantly increased early filling velocity (E) (1560±29 mm/s, p<0.0001 vs sham 1099±27 mm/s), rapid deceleration of the early filling wave (EDT) (15±0.5 ms, p<0.0001 vs sham 26±0.8 ms), and decreased atrial (A) filling velocity (271±24 mm/s, p<0.0001 vs sham 629±41 mm/s). Examples of pulsed-wave Doppler recordings of mitral inflow from a sham-operated rat and a rat with MI are shown in Fig.21B.

Ejection fraction was significantly improved in the C21 (0.03 mg/kg) (67±2 %, p<0.0001), C21 (0.3 mg/kg) (63±2 %, p<0.001), candesartan (61±2 %, p<0.001) and C21/candesartan treated group (62.3±3.7 %, p<0.001) compared to the vehicle group (49±2%).

Fractional shortening was significantly enhanced in C21(0.03 mg/kg) (39±1.8 %, p<0.001), C21(0.3 mg/kg) (35.1±1.7 %, p<0.001), candesartan (34.4±1.6 %, p<0.001) and C21/candesartan treated group (34.2±3 %, p<0.05) compared to vehicle group (26.1±1.6%).

The dilatation of LV (LVIDd) was significantly decreased in C21(0.03 mg/kg) (7.4±0.11 mm, p<0.0001), C21(0.3 mg/kg) (7.5±0.11 mm, p<0.0001), candesartan (7.8±0.09 mm, p<0.001) and C21/candesartan treated group (7.7±0.25 mm, p<0.05) compared to vehicle group (8.7±0.2 mm), (Fig. 21,22; Table 3).

Also diastolic function of the heart was significantly improved in all treated groups. E wave was significantly decreased in C21(0.03 mg/kg) (1197 ± 27 mm/s, $p<0.0001$), C21(0.3 mg/kg) (1040 ± 26 mm/s, $p<0.0001$), candesartan (1219 ± 42 mm/s, $p<0.0001$) and C21/candesartan treated group (1289 ± 33 mm/s, $p<0.0001$) compared to vehicle group (1560 ± 29 mm/s), (Fig. 21,22; Table 3).

A wave was significantly increased in C21(0.03 mg/kg) (586 ± 46 mm/s, $p<0.0001$), C21(0.3 mg/kg) (517 ± 31 mm/s, $p<0.0001$), candesartan (571 ± 45 mm/s, $p<0.0001$) and C21/candesartan treated group (576 ± 43 mm/s, $p<0.0001$) compared to vehicle group (271 ± 24 mm/s), (Fig. 21,22; Table 3).

EDT was significantly increased in C21(0.03 mg/kg) (22 ± 1 ms, $p<0.001$), C21(0.3 mg/kg) (20 ± 0.5 ms, $p<0.001$), candesartan (21 ± 1.5 ms, $p<0.001$) and C21/candesartan treated group (20 ± 0.8 ms, $p<0.001$) compared to vehicle group (15 ± 0.5 ms), (Fig. 21, 22; Table 3).

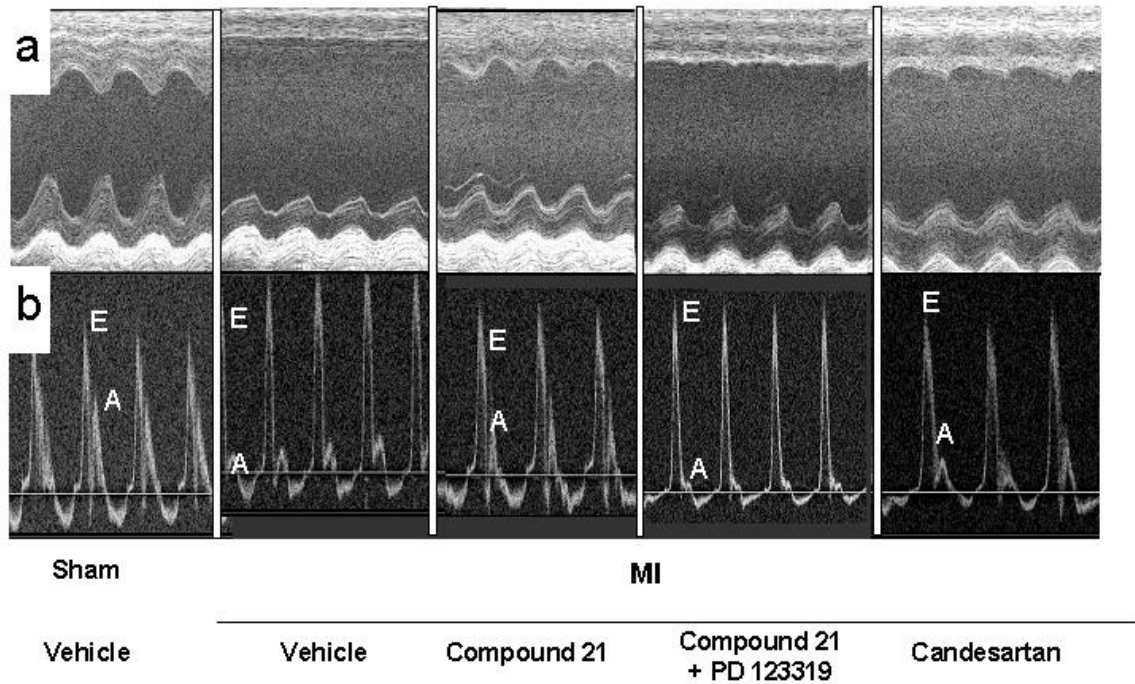


Figure 21: a) Representative M-mode echocardiograms. Note LV dilatation, thinning and akinesis of the anterior wall and hypokinesis of the posterior wall in vehicle treated rats after MI. C21 and Candesartan prevented LV dilatation and improved anterior and posterior wall motion. The effect of C21 was abolished by PD123319 co-treatment.

AW: anterior wall, PW: posterior wall

b) Representative pulsed-wave Doppler spectra of mitral inflow. Note increased E velocity, rapid deceleration of E wave and decreased A wave velocity in vehicle treated rats after MI. C21 and Candesartan treatment decreased E velocity, slowed deceleration of E wave and restored A wave velocity. The effect of C21 was abolished by PD123319 co-treatment.

E: peak velocity of early filling wave; A: peak velocity of late filling wave.

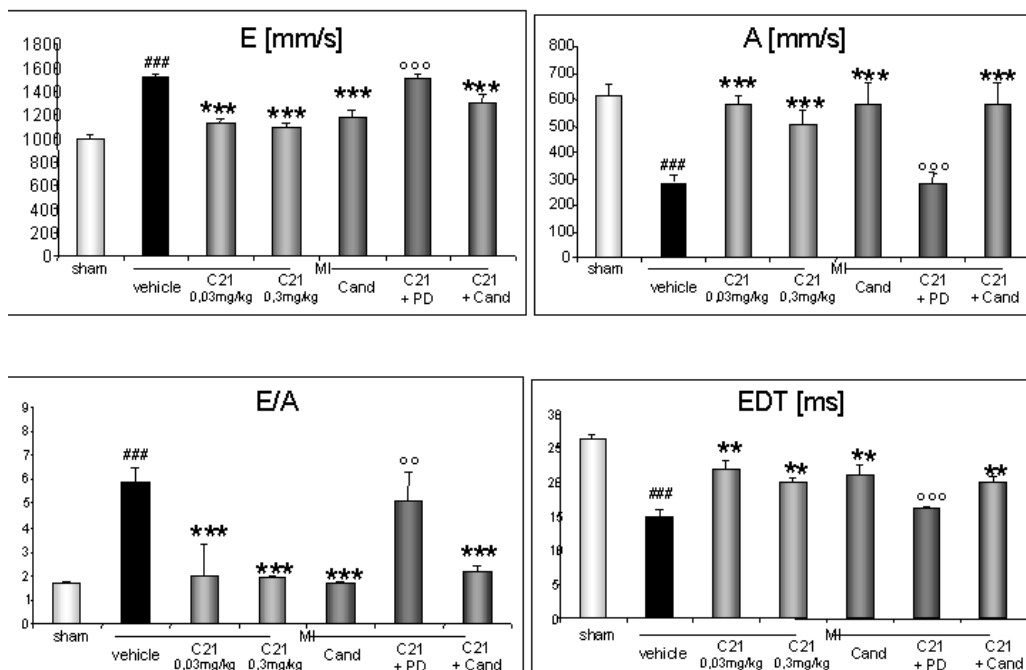
Also in the group with severe impairment of cardiac function (EF<35%) treated with C21 (0,3 mg/kg), all these parameters were significantly improved, the only exceptions being diastolic left ventricular inner diameter (8.8±0.19 mm vs vehicle 8.9±0.3 mm) and peak velocity of late filling wave (321± 68 mm/s vs vehicle 202± 21 mm/s), (Table 4).

The AT2R antagonist, PD 123319, completely or partly abolished the effects of C21 on LVIDd (8.1±0.3 mm vs C21 7.5±0.11 mm), LVIDs (6±0.3 mm, p<0.001 vs C21 4.3±0.12mm), FS (22.6±1.5 %, p<0.001 vs C21 35.1±1.7%), EF (43±2.4 %, p0.0001 vs C21 63±2%), E (1437±45 mm/s, p<0.0001 vs C21 1040±26 mm/s), A (285±44 mm/s, p<0.0001 vs C21 517±31 mm/s), and EDT (16.5± 0.7 ms, p<0.0001 vs C21 20± 0.5 ms), (Table 3; Fig.22).

Again, the combination of C21 and candesartan did not elicit any synergistic or additional effects.

The effect of C21 on post-infarct cardiac function was dose dependent: while 0,01 mg/kg was widely ineffective (data not shown), there was a significant improvement of cardiac function after treatment with 0.03 mg/kg which was only slightly and not in all cases further improved in animals treated with 0.3 mg/kg (Figure 22, Table 3).

Echocardiography



Echocardiography

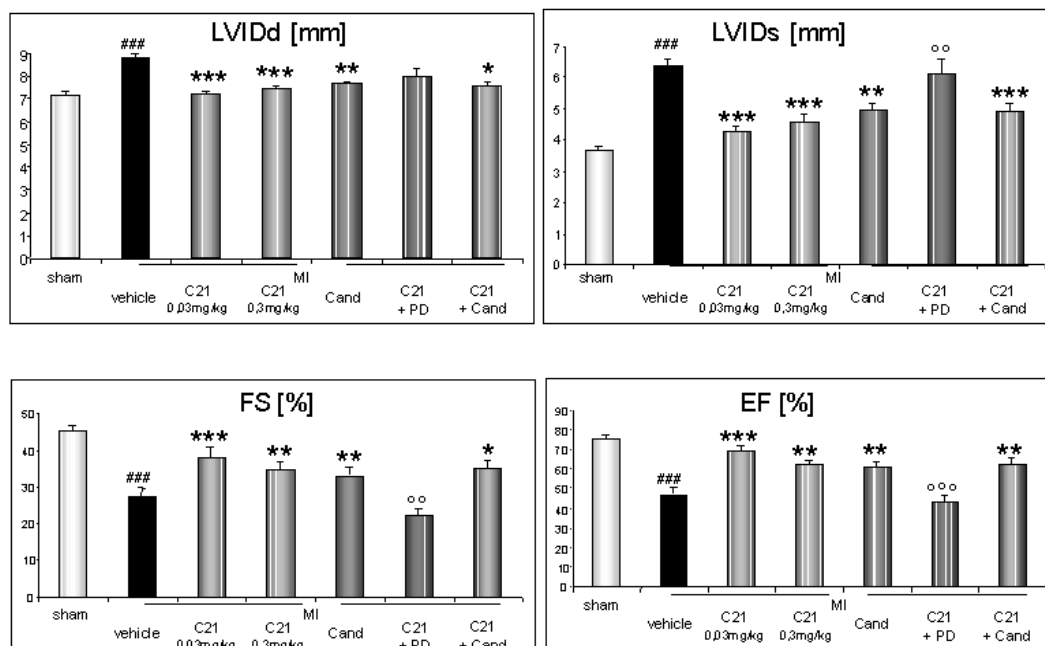


Figure 22: Hemodynamic parameters measured by echocardiography.

###p<0.0001 vs sham; ***p<0.0001 vs vehicle; **p<0.001 vs vehicle; *p<0.05 vs vehicle; ^{oo}p<0.0001 vs C21; ^{oo}p<0.001 vs C21

LVIDd: left ventricle internal dimension diastole, LVIDs: left ventricle internal dimension systole, FS: fractional shortening, EF: ejection fraction, E: peak velocity of early filling wave, A: peak velocity of late filling wave, EDT: deceleration time of E wave.

4.5 Inflammation Markers

Inflammation markers were measured a) in plasma and b) in cardiac tissue ex vivo.

a) Plasma MCP-1 (p<0.05) and MPO (p<0.001) were significantly increased in rats after MI compared to sham animals (Fig.23). In rats treated with C21, a significant reduction in MCP-1 (p<0.01) and MPO (p<0.01) levels could be noticed when compared to MI animals

b) The pro-inflammatory cytokines IL-1 β , IL-2 and IL-6 were determined by real time RT-PCR in the peri-infarct zone. Expression of all three cytokines was increased in hearts of MI/vehicle treated animals (IL-1 β : p<0.05, IL-2: p<0.05 and IL-6: p<0.01), (Fig.24) compared to sham animals. C21 treatment significantly reduced expression levels of IL-1 β : p<0.05), IL-2 (p<0.05) and IL-6 (p<0.01) compared to MI/vehicle. In this experimental setting, C21 proved to be as effective as the AT1R-antagonist, candesartan (IL-1 β : p<0.05, IL-2: p<0.05 and IL-6: p<0.01 vs MI/vehicle). The effect of C21 on IL-1 β and IL-6 expression could be inhibited by co-treatment of animals with the AT2R-antagonist PD 123319 (IL-1 β : p<0.05, IL-6: p<0,01). This effect was not observed for IL-2 expression, (Fig. 24).

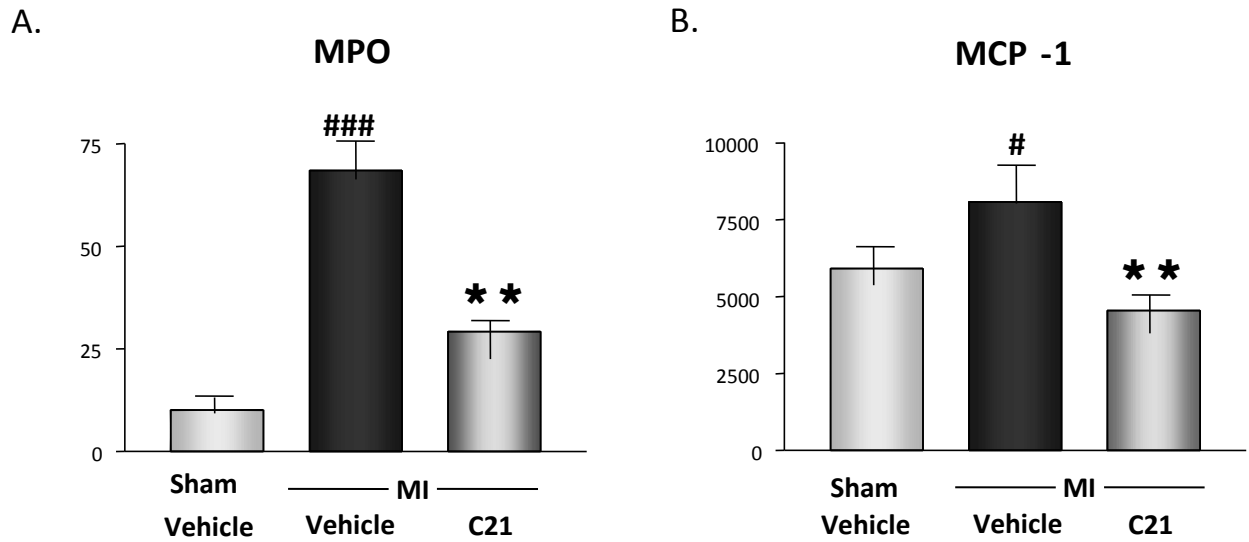


Figure 23:A. Myeloperoxidase (MPO) and B. Monocyte-chemoattractant protein-1 (MCP-1) levels in plasma estimated by ELISA. MI led to a significant increase in MPO and MCP-1 levels, which could be significantly reduced by C21 (C21; 0.03mg/kg/day i.p.) treatment (MPO: ###: $p < 0,001$ vs MI/vehicle; **: $p < 0,01$ vs MI/C21; MCP-1: #: $p < 0,05$ vs MI/vehicle, ** $p < 0,01$ vs MI/C21; $n = 6$ per group).

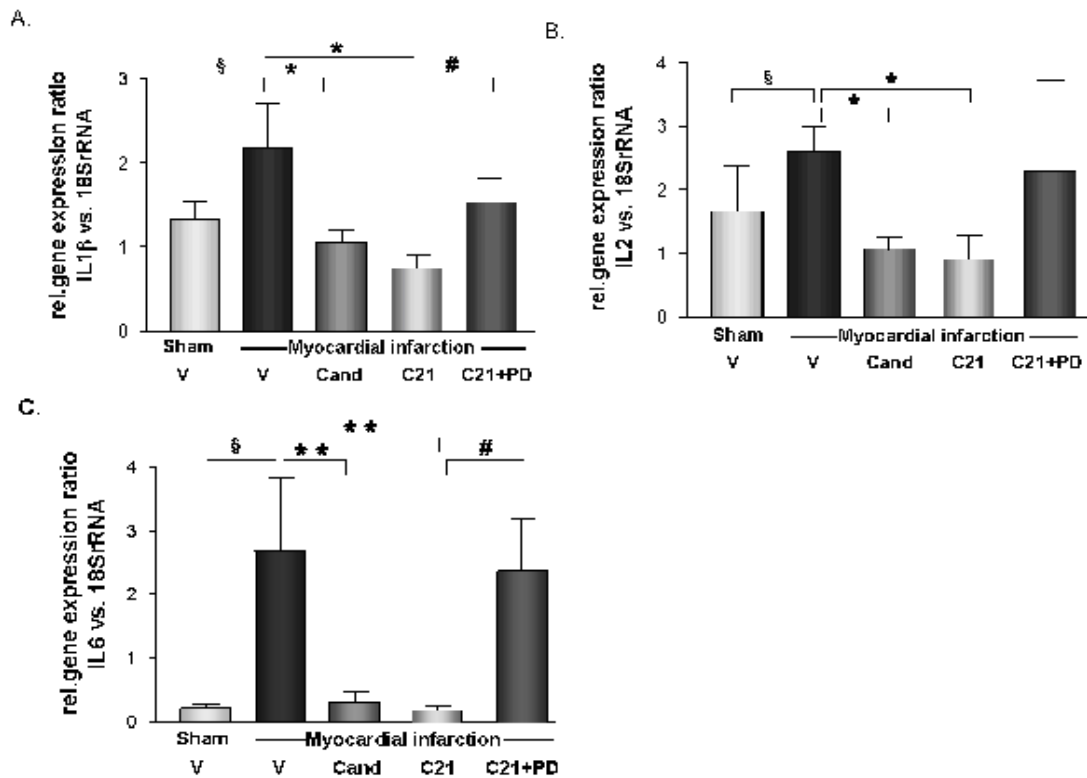


Figure 24: Expression of A) interleukin-1 β (IL-1 β), B) interleukin-2 (IL-2) and C) interleukin-6 (IL-6) in the peri-infarct zone in rat hearts. Myocardial infarction caused a significant increase in the expression of all cytokines examined (sham/vehicle vs MI/vehicle: $p < 0,05$ for IL-1 β (§), $p < 0,05$ for IL-2 (§), $p < 0,01$ for IL-6 (§§); $n = 6$ per group). Elevated expression levels were significantly reduced either by Candesartan (Cand; 0.1mg/kg/day i.p.) or by C21 (C21; 0.03mg/kg/day i.p.) treatment (MI/vehicle vs MI/Cand: $p < 0,05$ for IL-1 β (*), $p < 0,05$ for IL-2 (*), $p < 0,01$ for IL-6 (**); MI/vehicle vs MI/C21: $p < 0,05$ for IL-1 β (*), $p < 0,05$ for IL-2 (*), $p < 0,01$ for IL-6 (**); $n = 6$ per group). The effect of C21 was inhibited by co-treatment with PD123319 (PD; 3mg/kg/day i.p.) (MI/C21 vs MI/C21+PD: $p < 0,05$ for IL-1 β (#), non-significant for IL-2, $p < 0,01$ for IL-6 (##); $n = 6$ per group).

4.6 Apoptosis Markers

The apoptosis markers Fas-ligand and caspase 3 were measured in cardiac tissue (peri-infarct zone) by immunoblotting (Fig. 25). Myocardial infarction led to a significant increase in the expression of both markers compared to sham group.

C21 and candesartan reduced this increased expression to a comparable extent. The effect of C21 was blocked by the AT2R antagonist, PD 123319.

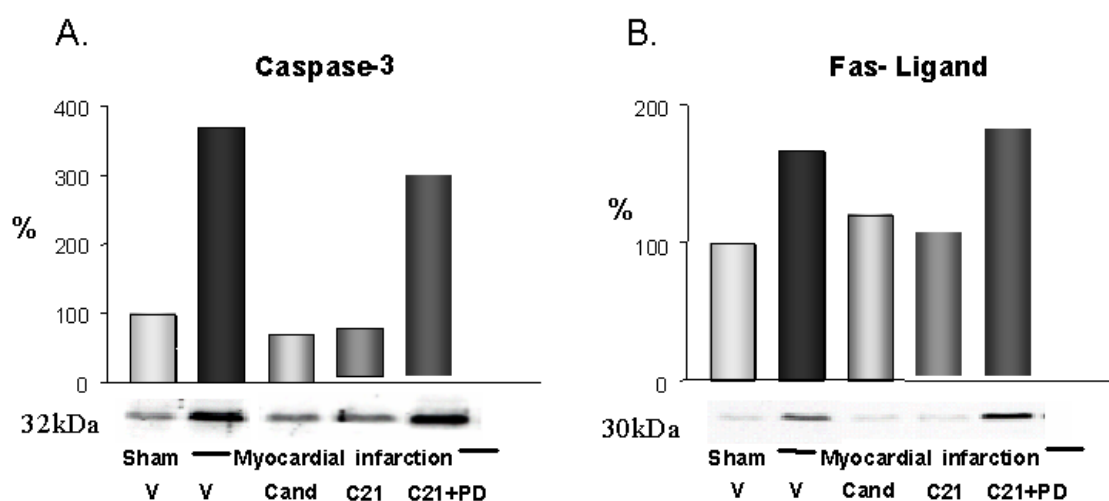
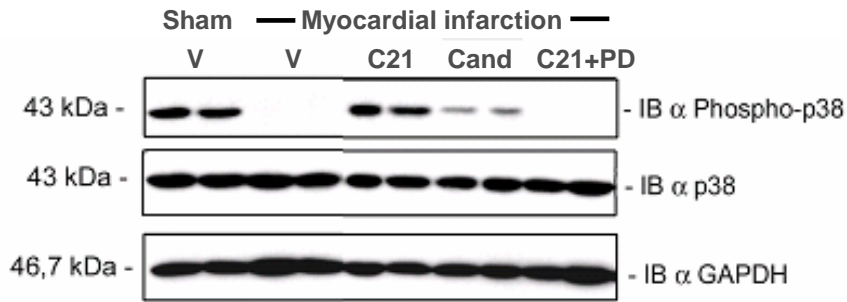


Figure 25: Western Blot analysis of A. caspase3- and B. Fas-ligand-expression in the peri-infarct zone of rat hearts. One representative of three blots for each marker is shown. Note the increase in caspase-3 and Fas-ligand expression after MI which was suppressed by candesartan (cand; 0.1mg/kg/day i.p.) or C21 (C21; 0.03mg/kg/day i.p.). Co-treatment with PD123319 (PD; 3mg/kg/day) blocked the effect of C21. V: vehicle.

A.



B.

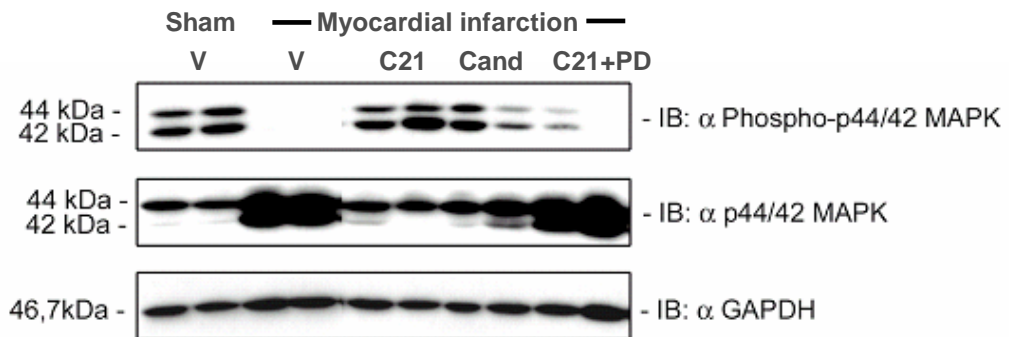


Figure 27: Western Blot analysis of A) phospho-p38-MAPK and B) phospho-p44/42-MAPK expression in the peri-infarct zone of rat hearts. One representative of three blots for each marker is shown. Note the complete loss of phospho-p38- and phospho-p44/42-MAPK expression after myocardial infarction. Phospho-p38- and phospho-p44/42-MAPK expression was only partly restored by candesartan (cand; 0.1mg/kg/day i.p.), while C21 (C21; 0.03mg/kg/day i.p.) led to an almost complete restoration of MAPK expression. Co-treatment with PD123319 (PD; 3mg/kg/day) blocked the effect of C21. V: vehicle.

4.9 Hemodynamic Measurements Obtained in Animals with Severe Post-infarct Impairment of Cardiac Function (EF<35%)

4.9.1 Millar Catheter

Hemodynamic parameters obtained on day 7 after MI/sham operation by Millar catheter in animals with severe post-infarct impairment of cardiac function (EF<35%) are presented in Table 4.

No significant change in the heart rate, left ventricular systolic pressure, or in the systolic or diastolic blood pressure was brought about by the treatment regimen or the surgical procedure.

In animals with severe post-infarct impairment of cardiac function, C21(0.03 mg/kg) still led to a significant improvement of LVEDP (11.6 ± 2.6 mmHg, $p < 0.005$ vs vehicle 23.9 ± 1.4 mmHg), contractility (92 ± 4 1/s, $p < 0.005$ vs vehicle 58 ± 8 1/s) and maxdP/dt (5997 ± 641 mmHg/s, $p < 0.05$ vs vehicle 3730 ± 476 mmHg/s), and tended to improve mindP/dt (4088 ± 599 mmHg/s vs vehicle 3200 ± 693 mmHg/s), (Table 4).

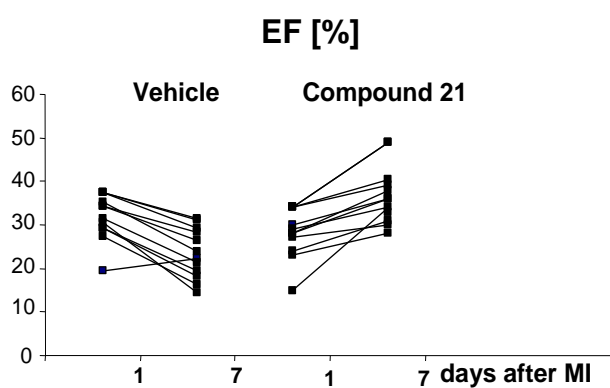


Figure 28: Change of EF in individual animals with EF<35% from treatment start (day 1) to end of treatment (day 7).

Table 4. Hemodynamics 7 days after MI in animals with severe impairment of cardiac function (EF ≤ 35%).

	Sham	MI	
		Vehicle	Comp 21 (0.03 mg/kg)
VSP, mmHg	131±9	101±7 [#]	110±11
LVEDP, mmHg	8.4±0.8	23.9±1.4 ^{###}	11.6±2.6 ^{**}
Contract.	105.8±5	58±8 ^{##}	92±4 ^{**}
maxdP/dt, mmHg/s	7850±576	3730±476 ^{###}	5997±641 [*]
mindP/dt, mmHg/s	6579±453	3200±693 ^{##}	4088±599
SBP, mmHg	120±8.7	100±7.5	112±11
DBP, mmHg	86±5.3	74±5	76±6
Pulse pressure	34.5±4	26±2	35±5
HR	248±7	245±7	229±16

VSP- left ventricular systolic pressure, LVEDP- left ventricular end diastolic pressure, Contractility: (maxdP/dt)/P, maxdP/dt- max peak rate of LV pressure, mindP/dt - min peak rate of LV pressure, SBP- systolic blood pressure, DBP- diastolic blood pressure, HR- heart rate.

###p < 0.0001 vs sham; ##p < 0.005 vs sham; **p < 0.005 vs vehicle ; *p < 0.05 vs vehicle

4.9.2 Transthoracic Doppler Echocardiography

Transthoracic echocardiography was performed 1 day after MI or sham operation to estimate EF before starting the treatment. There were no significant differences in EF between groups (Fig. 28).

Transthoracic Echocardiography was performed again 7 days after MI or sham operation to obtain systolic and diastolic function of the heart.

There were no changes in heart rate in the groups (Table 5).

Treatment with C21 (0.03 mg/kg) led to a significant improvement of ejection fraction ($40\pm 2.2\%$, $p < 0.0005$ vs vehicle $19\pm 2\%$) and fractional shortening ($20.7\pm 1.3\%$, $p < 0.0005$ vs vehicle $9.4\pm 2\%$).

The systolic left ventricular inner diameter was significantly decreased in C21 treated group (6.9 ± 0.2 mm, $p < 0.05$ vs vehicle 8 ± 0.2 mm).

Also the diastolic heart function was significantly enhanced in C21 treated group: peak velocity of early filling wave (1271 ± 69 mm/s, $p < 0.0005$ vs vehicle 1691 ± 40 mm/s), deceleration time (23 ± 2 , $p < 0.005$ ms vs vehicle 12.8 ± 1 ms) and E/A (4.3 ± 0.8 , $p < 0.05$ vs vehicle 8.4 ± 1.2), (Table 5).

Table 5. Transthoracic Doppler Echocardiography measurements 7 days after MI in animals with severe impairment of cardiac function ($EF \leq 35\%$).

	Sham	MI	
		Vehicle	Comp 21 (0.03 mg/kg)
LVIDd, mm	6.9 ± 0.16	$8.9\pm 0.3^{###}$	$8.8\pm 0.19^{###}$
LVIDs, mm	3.7 ± 0.14	$8\pm 0.2^{###}$	$6.9\pm 0.2^{###*}$
FS, %	45.5 ± 1.4	$9.4\pm 2^{###}$	$20.7\pm 1.3^{###***}$
EF, %	76 ± 1.3	$19\pm 2^{###}$	$40\pm 2.2^{###***}$
E, mm/s	1105 ± 36	$1691\pm 40^{###}$	$1271\pm 69^{***}$
A, mm/s	648 ± 40	$202\pm 21^{###}$	$321\pm 68^{##}$
E/A	1.7 ± 0.07	$8.4\pm 1.2^{###}$	$4.3\pm 0.8^{##*}$
EDT, ms	26.4 ± 0.6	$12.8\pm 1^{###}$	$23\pm 2^{**}$
HR	369 ± 15	363 ± 8	352 ± 21

LVIDd- left ventricular internal dimension end diastole, LVIDs- left ventricular internal dimension end systole, FS- fractional shortening, EF- ejection fraction, E- peak velocity of early filling wave, A- peak velocity of late filling wave, EDT- E wave deceleration time, HR- heart rate. $### p < 0.0001$ vs sham; $*** p < 0.0005$ vs vehicle ; $** p < 0.005$ vs vehicle ; $* p < 0.05$ vs vehicle

DISCUSSION

While it is unanimously accepted that stimulation of angiotensin AT1Rs contributes to tissue damage, inflammation and unfavorable tissue remodeling after MI, data about the role of AT2R in this context are controversial (Widdop et al., 2003). This is certainly due to the fact that until now practicable and reliable tools to study AT2R actions by direct AT2R stimulation have not been available: Treatment with the natural ligand angiotensin II (Ang II) mostly elicits effects mediated by the dominating AT1R, the only available AT2R antagonist, PD 123319, is unselective at higher doses (Macari et al., 1993), and the only available AT2R agonist, CGP 42112, is a peptide so it is rapidly degraded in vivo and, furthermore, has agonistic and antagonistic properties, which renders the interpretation of in vivo data difficult (Stoll et al., 1995). A further obstacle to obtaining clear experimental results on AT2R function was the fact that this receptor, despite belonging to the large family of so-called seven transmembrane domain receptors usually coupled to G-proteins, associates directly but alternatively with at least three intracellular binding proteins, a phosphatase (SHP-1), ATBP/ATIP and PLZF, each initiating a distinct signaling pathway engendering different cellular and functional responses (Funke-Kaiser et al., 2009).

Despite all these difficulties leading to some controversies over the physiological and pathophysiological role of AT2R in the adult organism, a certain picture has emerged over the years favoring antiproliferative rather than proliferative or hypertrophic actions, anti-inflammatory rather than inflammatory and anti-apoptotic rather than apoptotic action (de Gasparo et al., 2000; Jones ES et al., 2008; Steckelings UM et al., 2005; Rehman et al., 2012).

This is the first in vivo study using a specific and selective, non-peptide, orally active AT2R agonist, C21. For the first time, this agonist allows direct in vitro and in vivo stimulation of AT2R without affecting AT1R. In addition, this pharmacological approach may give rise to agonist concentrations at the receptor site far exceeding those previously achieved by the natural ligand, Ang II, by a factor of more than 1,000 without compromising selectivity.

MI was induced in normotensive Wistar rats by permanent ligation of the left anterior descending coronary artery. Subsequently, animals were treated with C21 for one week. Direct AT2R stimulation by C21 improved systolic and diastolic cardiac function post MI coinciding with a smaller infarct scar in C21 treated animals compared to vehicle treatment. While MI led to an impairment of all parameters measured by echocardiography (LVIDs, EF, FS for systolic function; LVIDd, E, A, E/A, EDT for diastolic function) or Millar catheter (contractility, maxdP/dt for systolic function; LVEDP, mindP/dt for diastolic function), respectively, treatment with C21 improved all of these parameters. For most parameters, the effect of C21 could be inhibited by co-treatment with the established AT2R antagonist, PD 123319, thus providing good evidence that the effects seen by C21 treatment are indeed a result of specific AT2R stimulation.

Apart from rats treated with different doses of C21, our study also included a group of animals treated with the AT1R antagonist candesartan. We used an AT1R antagonist as a reference drug (a) because of its proven efficacy in the improvement of post-infarct cardiac function as shown in animals and clinically and (b) because it may interfere with the RAAS at least in part by indirect AT2R stimulation. We did not intend to compare the efficacy but rather the quality of actions of the two drugs, because at present – with only very limited data and experimental experience with C21 available - it is hard to define what an equally effective dose of C21 or candesartan would be. Nevertheless, in mild to moderate infarctions, both drugs restored a number of cardiac parameters back to levels in non-infarcted animals; i.e. with regard to these parameters, both drugs elicited an equal, maximal response (E, A, E/A, EDT). Regarding those parameters, in which a maximal response was not achieved thus allowing a “comparison” of C21 and candesartan actions (LVIDs, LVIDd, EDP, contractility, mindP/dt), the improvement with C21 was more effective than with candesartan. This outcome applied to systolic and diastolic function, and may point to a superiority of C21. The outcome of animals treated with the combination of C21 plus candesartan was not superior to that of animals treated with C21 alone as may have been expected. A likely reason for this finding could be that C21 mono-therapy already elicited a maximal functional improvement – not allowing for any further improvement.

In order to get a tentative idea about the molecular mechanisms underlying the beneficial effect of C21 on post-MI cardiac function, we looked for a putative effect of this drug on the apoptotic and inflammatory response in the peri-infarct zone.

MI led to a significant increase in Fas-ligand and caspase-3 expression in the infarct border zone. C21 significantly reduced the elevated, MI-related Fas-ligand and caspase-3 expression, and this effect could be blocked by the specific AT2R-antagonist, PD 123319. Because apoptosis is a major contributor in post-infarct cardiac remodeling, including the development of infarct expansion (Diwan et al., 2007), prevention of cardiomyocyte apoptosis by C21 may be a major molecular mechanism by which AT2-R stimulation preserves cardiac function after MI.

The mitogen-activated protein kinases (MAPK) are involved in numerous cellular processes such as apoptosis, inflammation, proliferation or hypertrophy. In our study we found that the activity of p38 MAPK and p44/42 MAPK was reduced to undetectable levels 7 days after MI in vehicle treated animals, and that treatment with C21 was able to completely restore p38 MAPK and p44/42 MAPK expression in infarcted hearts. This effect was blocked by PD 123319 indicating again AT2R specificity of the C21 effect. The effect of candesartan was by far weaker than that of C21.

While MAPKs have traditionally been regarded as mediators of e.g. proliferation, apoptosis and inflammation, recent data provided evidence that MAPK activation can also result in beneficial effects directly opposed to the ones described above, namely anti-proliferation, cell survival and anti-inflammation (Lips et al., 2004). In our experimental setting, the rescue

of p38 MAPK and p44/42 MAPK expression by C21 seven days after MI coincided with an improvement of cardiac function and a smaller scar size. Although this is just an observation of coincidence, a causal relationship between MAPK activation and improved cardiac function is supported by a recent study by Tenhunen et al. (2006), in which the authors were able to improve post-infarct cardiac function by rescuing p38 MAPK expression through local adenovirus-mediated p38 MAPK gene transfer. Functionally, MAPK rescue reduced fibrosis and apoptosis (the latter shown by TUNEL staining and – like in our study – by a reduction of caspase-3). Thus, the increase in p38 and p44/42 MAPK expression by C21 may be part of its anti-apoptotic effect after MI, which is also reflected by a decrease in caspase-3 and Fas-ligand.

Already studies using the peptide AT2R agonist CGP42112A showed an anti-inflammatory effect of AT2R which contributes to its tissue protective property. Three signaling mechanisms mediating anti-inflammation have been defined for AT2R: inhibition of JAK/STAT signaling (Horiuchi et al., 1999), inhibition of NF- κ B (Wu et al., 2004) and inhibition of COX2 synthesis (Tani et al., 2008), the latter two by means of AT2R stimulation with CGP42112A.

In the early phase after acute MI, necrosis of cardiac cells sets into motion an inflammatory response which ultimately promotes fibrosis, scar formation and thereby heart failure. C21 suppressed this post-infarct inflammatory response as shown by a significant decrease in cytokine (MCP-1, IL-1 β , IL-2, IL-6) expression in plasma and the peri-infarct zone. Again, the effect of C21 could be blocked by the AT2R antagonist indicating AT2R- specificity of this effect. Since it has been shown for other drugs that inhibition of the inflammatory response contributes to the preservation of cardiac function, it can be assumed that anti-inflammation may be another mechanism of action of AT2R- stimulation by C21.

It has to be pointed out that this study was performed in normotensive rats, and that there were no changes in blood pressure or heart rate over the course of the experiment: neither by C21 at all doses used, nor by candesartan which was given in a non blood pressure lowering dose. Therefore, the effects on cardiac function, cytokine- and apoptosis-markers as well as MAPK expression are unlikely to be caused by treatment-related hemodynamic changes. This notion is further supported by the inhibitory effect of C21 on IL-6 expression in rat fetal cardiomyocytes in vitro, i.e. in an experimental setting independent of any hemodynamic influences.

5.1 Conclusion

Taken together, this is the first study using a non-peptide AT2R-agonist for direct stimulation of AT2R after myocardial infarction in rats. Treatment with C21 over a period of 6 days led to a pronounced improvement of systolic and diastolic cardiac function accompanied by a smaller scar volume. Furthermore, C21 reduced apoptosis and showed an anti-inflammatory action, suggesting that these are mechanisms contributing to the beneficial effect of AT2R stimulation.

5.2 Limitations

Because in our study the infarct size was measured at the end but not before treatment, we cannot exclude an unmeasured difference in infarct size between groups at baseline, which may have influenced the outcome of the study. However, this possibility was minimized by grouping animals according to EF before the start of treatment to keep differences in mean EF between groups minimal. This procedure is based on the observation by us and others that EF correlated well with infarct size ($r^2 < 0.671$; $P < 0.0001$) (Sciagra et al., 2004).

Moreover, assignment of animals to the respective treatment groups was performed by an investigator who was blinded to the outcome of EF measurement in individual animals (only knowing whether EF was $>35\%$ or $<35\%$).

Clinical Relevance

Interference with the RAAS is a very common, well established and successful concept of treatment in cardiovascular disease. All currently available and approved RAAS-interfering drugs (ACE inhibitors, AT1R blockers, renin inhibitors, aldosterone antagonists) aim at inhibiting the unfavorable effects of an overactivated RAAS signaling via AT1R. However, the RAAS does not only harbor the renin-ACE-AT1R-aldosterone-axis, which, when overstimulated, is involved in a huge variety of pathologies ranging from hypertension to end organ damage or local processes in myocardial infarction and stroke. In fact, it also possesses a tissue-protective axis involving monoxycarboxypeptidase angiotensin-converting enzyme 2 (ACE2), Ang-(1-7) produced through hydrolysis of Ang II, and the Mas receptor and the AT2R which seems to counteract detrimental effects mediated by AT1R. Evidence suggests that a reduction in the expression and activity of this vasodepressor component may be a critical factor in mediating the progression of cardiovascular disease (Ferrario et al., 2011).

At present, there is no pharmacological tool available to specifically stimulate this beneficial ACE2-Ang1-7-AT2R-axis in vivo. The novel non-peptide AT2R-agonist C21 may be such a drug. The study presented here is the first to test the therapeutic potential of direct AT2R stimulation in a model of myocardial infarction. C21 significantly improved cardiac function and resulted in a smaller scar size independent of any hemodynamic changes. Since C21 is a non-peptide with a sufficient bioavailability (approx. 30%), it may be a suitable lead compound for the development of a drug for blood-pressure independent treatment or prevention of end organ damage in human.

References

Adachi Y, Saito Y, Kishimoto I, Harada M, Kuwahara K, Takahashi N, Kawakami R, Nakanishi M, Nakagawa Y, Tanimoto K, Saitoh Y, Yasuno S, Usami S, Iwai M, Horiuchi M, Nakao K. *Angiotensin II Type 2 Receptor Deficiency Exacerbates Heart Failure and Reduces Survival After Acute Myocardial Infarction in Mice*. *Circulation* 2003;107;2406-2408

Bedecs K, Elbaz N, Sutren M, Masson M, Susini C, Strosberg AD, et al. *Angiotensin II type 2 receptors mediate inhibition of mitogen-activated protein kinase cascade and functional activation of SHP-1 tyrosine phosphatase*. *Biochem J* 1997;325(Pt 2):449–54.

Bosnyak, IK Welungoda, A Hallberg, M Alterman, RE Widdop and ES Jones. *Stimulation of angiotensin AT 2 receptors by the non-peptide agonist, Compound 21, evokes vasodepressor effects in conscious spontaneously hypertensive rats*. *British Journal of Pharmacology* 2010,159, 709–716.

Bove CM, Yang Z, Gilson WD, Epstein FH, French BA, Berr SS, Bishop SP, Matsubara H, Carey RH, Kramer CM. *Nitric oxide mediates benefits of angiotensin II type 2 receptor overexpression during post-infarct remodeling*. *Hypertension*. 2004 ;43:680-685.

Bove CM, Gilson WD, Scott CD, Epstein FH, Yang Z, Dimaria JM, Berr SS, French BA, Bishop SP, Kramer CM. *The angiotensin II type 2 receptor and improved adjacent region function post-MI*. *J Cardiovasc Magn Reson*. 2005;7:459-464.

Carey RM, Wang ZQ, Siragy HM. *Role of the angiotensin type 2 receptor in the regulation of blood pressure and renal function*. *Hypertension* 2000;35:155–63.

de Gasparo M, Catt KJ, Inagami T, Wright JW, Unger T. International union of pharmacology. XXIII. *The angiotensin II receptors*. *Pharmacol Rev* 2000;52:415–72.

Fei Jing, Masaki Mogi, Akiko Sakata, Jun Iwanami, Kana Tsukuda, Kousei Ohshima, Li-Juan Min, Ulrike M Steckelings, Thomas Unger, Björn Dahlöf and Masatsugu Horiuchi. *Direct stimulation of angiotensin II type 2 receptor enhances spatial memory*. *Journal of Cerebral Blood Flow and Metabolism* 2012; 32:248-255.

Ferrario CM. *ACE2: more of Ang-(1-7) or less Ang II?*. *Curr Opin Nephrol Hypertens*. 2011 20(1):1-6

Funke-Kaiser H, Reinemund J, Steckelings UM, Unger T. Signal transduction and regulation of the angiotensin type 2 receptor (AT2) – implications for cardiac pathophysiology. *J Renin Angiotensin Aldosterone Syst* 2009.

Gallinat S, Busche S, Schütze S, Krönke M, Unger T. *AT2 receptor stimulation induces generation of ceramides in PC12W cells.* *FEBS Lett* 1999;443:75–9.

Geisterfer AA, Peach MJ, Owens GK. *Angiotensin II induces hypertrophy, not hyperplasia, of cultured rat aortic smooth muscle cells.* *Circ Res* 1988; 62:749–856.

Gigante B, Rubattu S, Russo R, Porcellini A, Enea I, De Paolis P, et al. *Opposite feedback control of renin and aldosterone biosynthesis in the adrenal cortex by angiotensin II AT1-subtype receptors.* *Hypertension* 1997; 30:563–568.

Griendling KK, Minieri CA, Ollerenshaw JD, Alexander RW. *Angiotensin II stimulates NADH and NADPH oxidase activity in cultured vascular smooth muscle cells.* *Circ Res* 1994; 74:1141–1148.

Hannan RE, Gaspari TA, Davis EA, Widdop RE. *Differential regulation by AT(1) and AT(2) receptors of angiotensin II-stimulated cyclic GMP production in rat uterine artery and aorta.* *Br J Pharmacol* 2004;141:1024–31.

Horiuchi M, Hayashida W, Kambe T, Yamada T, Dzau VJ. *Angiotensin type 2 receptor dephosphorylates Bcl-2 by activating mitogen-activated protein kinase phosphatase-1 and induces apoptosis.* *J Biol Chem* 1997;272:19022–6.

Huang XC, Richards EM, Sumners C. *Angiotensin II type 2 receptor-mediated stimulation of protein phosphatase 2A in rat hypothalamic/brainstem neuronal cocultures.* *J Neurochem* 1995;65:2131–7.

Ichihara S, Senbonmatsu T, Price E Jr, Ichiki T, Gaffney FA, Inagami T. *Targeted deletion of angiotensin II type 2 receptor caused cardiac rupture after acute myocardial infarction.* *Circulation.* 2002; 106:2244-2249

Kang J, Posner P, Sumners C. *Angiotensin II type 2 receptor stimulation of neuronal K⁺ currents involves an inhibitory GTP binding protein.* *Am J Physiol* 1994;267:1389.

Kaschina E, Unger T. *Angiotensin AT1/AT2 receptors: regulation, signalling and function.* *Blood Press.* 2003;12(2):70-88. Review.

Krämer, S; Peters, H; Mika, A; Loof, T; Althoff, N; Neumayer, H; Unger, T; Steckelings, UM. *The Non-Peptide At2-Receptor Agonist Compound 21 Ameliorates Hypertrophy and Fibrosis in Uremia-Associated Cardiomyopathy: 9D.04.* *Journal of Hypertension.* 2010;28(7)442.

Li D-Y, Tao L, Liu H, Christopher TA, Lopez BL, Ma XL. *Role of ERK1/2 in the anti-apoptotic and cardioprotective effects of nitric oxide after myocardial ischemia and reperfusion*. *Apoptosis*. 2006; 11: 923–930.

Lips DJ, Bueno OF, Wilkins BJ, Purcell NH, Kaiser RA, Lorenz JN, Voisin L, Saba-El-Leil MK, Meloche S, Pouysségur J, Pagès G, De Windt LJ, Doevendans PA, Molkentin JD. *MEK1-ERK2 signaling pathway protects myocardium from ischemic injury in vivo*. *Circulation*. 2004;109:1938-1941.

Litwin SE, Katz SE, Morgan JP, Douglas PS: *Serial Echocardiographic Assessment of Left Ventricular Geometry and Function After Large Myocardial Infarction in the Rat*. *Circulation*. 1994;89:345-354.

Lucinda M. Hilliard, Emma S. Jones, U. Muscha Steckelings, Thomas Unger, Robert E. Widdop, Kate M. Denton. *Sex-Specific Influence of Angiotensin Type 2 Receptor Stimulation on Renal Function*. *Hypertension*. 2012; 59: 409-414.

Macari D, Bottari SP, Whitebread S, De Gasparo M, Levens N. *Renal actions of the selective angiotensin AT2 receptor ligands CGP 42112B and PD 123319 in the sodium-depleted rat*. *Eur J Pharmacol*. 1993;249:85-93.

Miura S, Karnik SS, Saku K. *Constitutively active homo-oligomeric angiotensin II type 2 receptor induces cell signaling independent of receptor conformation and ligand stimulation*. *J Biol Chem*. 2005; 280:18237-18244.

Naftilan AJ, Pratt RE, Dzau VJ. *Induction of platelet-derived growth factor A-chain and c-myc gene expressions by angiotensin II in cultured rat vascular smooth cells*. *J Clin Invest* 1989; 83:1419–1424.

Nakajima M, Hutchinson HG, Fujinaga M, Hayashida W, Morishita R, Zhang L, Horiuchi M, Pratt RE, Dzau VJ. *The angiotensin II type 2 (AT2) receptor antagonizes the growth effects of the AT1 receptor: gain-of-function study using gene transfer*. *Proc Natl Acad Sci U S A*. 1995; 92:10663–10667.

Navar LG, Inscho EW, Majid SA, Imig JD, Harrison-Bernard LM, Mitchell KD. *Paracrine regulation of the renal microcirculation*. *Physiol Rev* 1996;76:425–536.

Nio Y, Matsubara H, Murasawa S, Kanasaki M, Inada M: *Regulation of gene transcription of angiotensin II receptor subtypes in myocardial infarction*. *J Clin Invest*. 1995; 95:46-54.

Oishi Y, Ozone R, Yano Y, Teranishi Y, Akishita M, Horiuchi M, Oshima T, Kambe M. *Cardioprotective role of AT2 receptor in postinfarction left ventricular remodeling*. Hypertension. 2003; 41:814-818.

Oishi Y, Ozone R, Yoshizumi M, Akishita M, Horiuchi M, Oshima T. *AT2receptor mediates the cardioprotective effects of AT1 receptor antagonist in post-myocardial infarction remodeling*. Life Sci. 2006; 80:82-88.

Pfeffer MA, McMurray JJV, Velazquez EJ, Rouleau J-L, Kober L, Maggioni AP, Solomon SD, Swedberg K, Van de Werf F, White H, Leimberger JD, Henis M, Edwards S, Zelenkofske S, Sellers MA, Califf RM. *Valsartan, Captopril, or Both in Myocardial Infarction Complicated by Heart Failure, Left Ventricular Dysfunction, or Both*. New Engl J Med. 2003; 349:1893-1906.

Raij L. *Hypertension and cardiovascular risk factors: role of the angiotensin II–nitric oxide interaction*. Hypertension 2001; 37:767–773.

Rajagopalan S, Kurz S, Munzel T, Tarpey M, Freeman BA, Griending KK, Zafari AM, Ushio-Fukai M, Minieri CA, Akers M, Lassegue B, Griending KK. *Arachidonic acid metabolites mediate angiotensin II-induced NADH/NADPH oxidase activity and hypertrophy in vascular smooth muscle cells*. Antioxidants Redox Signaling 1999; 1:167–179.

Rehman, Leibowitz, Yamamoto, Rautureau, Paradis, Schiffrin. *Angiotensin Type 2 Receptor Agonist Compound 21 Reduces Vascular Injury and Myocardial Fibrosis in Stroke-Prone Spontaneously Hypertensive Rats*. Hypertension 2012; 59: 291-299.

Ruiz-Ortega M, Lorenzo O, Ruperez M, Esteban V, Suzuki Y, Mezzano S, et al. *Role of the renin–angiotensin system in vascular diseases: expanding the field*. Hypertension 2001; 38:1382–1387.

Speth, R. C.; Kim, K. H. *Discrimination of two angiotensin II receptor subtypes with a selective agonist analogue of angiotensin II, p-aminophenylalanine⁶ angiotensin II*. Biochem. Biophys. Res. Commun. 1990, 169, 997-1006.

Steckelings UM, Kaschina E, Unger Th. *The AT2-receptor: a matter of love and hate*. Peptides. 2005; 26:1401-1409.

Stoll M, Steckelings UM, Paul M, Bottari SP, Metzger R, Unger Th. *The angiotensin AT2-receptor mediates inhibition of cell proliferation in coronary endothelial cells*. J Clin Invest. 1995; 95:651-657.

Taubman MB, Berk BC, Izumo S, Tsuda T, Alexander RW, Nadal-Ginard B. *Angiotensin II induces c-fos mRNA in aortic smooth muscle: role of Ca²⁺ mobilization and protein kinase C activation.* J Biol Chem 1989;264:526–530.

Tenhunen O, Soini Y, Ilves M, Rysa J, Tuukkanen J, Serpi R, Pennanen H, Ruskoaho H, Leskinen H. *p38 Kinase rescues failing myocardium after myocardial infarction: evidence for angiogenic and antiapoptotic mechanisms* FASEB J. 2006; 20: E1276–E1286.

Touyz RM, Chen X, Tabet F, Yao G, He G, Quinn MT, et al. *Expression of a functionally active gp91phox-containing neutrophil-type NAD(P)H oxidase in smooth muscle cells from human resistance arteries. Regulation by angiotensin II.* Circ Res 2002; 90:1205–1213.

Unger T. *The angiotensin type 2 receptor: variations on an enigmatic theme.* J Hypertens 1999;17:1775–86.

Volpe M, Musumeci B, de Paolis P, Savoia C, Morganti A. *Angiotensin II AT₂ receptor subtype: an uprising frontier in cardiovascular disease?* J Hypertens.2003; 21:1429-1443.

Voros S, Yang Z, Bove CM, Gilson WD, Epstein FH, French BA, Berr SS, Bishop SP, Conaway MR, Matsubara H, Carey RM, Kramer CM. *Interaction between AT₁ and AT₂ receptors during postinfarction left ventricular remodeling.* Am J Physiol Heart Circ Physiol. 2006; 290:H1004-1010.

Wan Y, Wallinder C, Plouffe B, Beaudry H, Mahalingam AK, Wu X, Johansson B, Holm M, Botoros M, Karlen A, Pettersson A, Nyberg F, Fändriks L, Gallo-Payet N, Hallberg A, Alterman M. *Design, synthesis, and biological evaluation of the first selective nonpeptide AT₂ receptor agonist.* J Med Chem 2004; 47:5995-6008.

Whitebread, S.; Mele, M.; Kamber, B.; de Gasparo, M. *Preliminary biochemical characterization of two angiotensin II receptor subtypes.* Biochem. Biophys. Res. Commun. 1989, 163, 284-291.

Widdop RE, Jones ES, Hannan RE, Gaspari TA. *Angiotensin AT₂ receptors: cardiovascular hope or hype?* Br J Pharmacol. 2003; 140:809–824.

Wu L, Iwai M, Nakagami H, Chen R, Suzuki J, Akishita M, et al. *Effect of angiotensin II type 1 receptor blockade on cardiac remodeling in angiotensin II type 2 receptor null mice.* ArteriosclerThromb Vasc Biol 2002;22:49–54.

Wu L, Iwai M, Nakagami H, Li Z, Chen R, Suzuki J, et al. *Roles of angiotensin II type 2 receptor stimulation associated with selective angiotensin II type 1 receptor blockade with valsartan in the improvement of inflammation-induced vascular injury.* Circulation 2001;104:2716–21.

Xu J, Carretero OA, Liu YH, Shesely EG, Yang F, Kapke A, Yang XP. *Role of AT2 receptors in the cardioprotective effect of AT1 antagonists in mice.* Hypertension. 2002; 40:244-250.

Yang Z, Bove CM, French BA, Epstein FH, Berr SS, DiMaria JM, Gibson JJ, Carey RM, Kramer CM. *Angiotensin II type 2 receptor overexpression preserves left ventricular function after myocardial infarction.* Circulation. 2002 ;106:106-111.

Zhuo J, Alcorn D, Allen AM, Mendelsohn FA. *High resolution localization of angiotensin II receptors in rat renal medulla.* Kidney Int 1992; 42:1372–1380.

Zhuo J, McGregor DP, Mendelsohn FAO. *Comparative distribution of angiotensin II receptor subtypes in mammalian adrenal glands. In: Vinson GP, Anderson DC (editors): Adrenal glands, vascular system and hypertension.* Melbourne: Journal of Endocrinology; 1996, pp. 53–68.

CURRICULUM VITAE

"Mein Lebenslauf wird aus datenschutzrechtlichen Gründen in der elektronischen Version meiner Arbeit nicht veröffentlicht."

Erklärung

„Ich, Aleksandra Grzesiak, erkläre, dass ich die vorgelegte Dissertation mit dem Thema: Angiotensin II type 2 receptor stimulation. A novel options of therapeutic interference with the renin-angiotensin system in myocardial infarction? selbst verfasst und keine anderen als die angegebenen Quellen und Hilfsmittel benutzt, ohne die (unzulässige) Hilfe Dritter verfasst und auch in Teilen keine Kopien anderer Arbeiten dargestellt habe.“

16.10.2012

Unterschrift

Published Abstracts

1. Kruger F, Kappert K, Foryst-Ludwig A, Clemenz M, **Grzesiak A**, Sommerfeld M, Kemnitz UR, Unger Th, Kaschina E. *Telmisartan attenuates outward aortic remodelling associated with diet –induced obesity*. Hypertension 52 (4): 757, 2008
2. Brinckmann MP, Timm M, Kaschina E, Altarche-Xifro W, **Grzesiak A**, Curato C, Unger T, Li J. *ERa is expressed in cardiac c-kit plus cells and supports self-renewal after cardiac ischemic injury in rat*. Circulation 118 (12) : 246
3. Altarche-Xifro W, Birka C, Kaschina E, Timm M, **Grzesiak A**, Curato C, Brinckmann MP, Unger T, Li J. *Angiotensin AT2 receptor mediates cardiac c-kit plus cell proliferation and supports survival of cardiomyocyte*. Circulation 118 (12) : 436-437
4. **Grzesiak A**, Kaschina E, Foryst-Ludwig A. et al. *AT2-receptor stimulation: A novel option of therapeutic interference with the renin-angiotensin-system in myocardial infarction*. Journal of Hypertension 26: S19-S13 Suppl. 1, 2008
5. Kaschina E, Schrader F, Sommerfeld M, Kemnitz UR, **Grzesiak A**, Krikov M, Unger T. *Telmisartan prevents aneurysm formation in the rat independently of blood pressure reduction by inhibiting proteolysis, apoptosis and inflammation*. Journal of Hypertension 26: S170-S170 Suppl. 1, 2008
6. Altarche-Xifro W, Birka C, Kaschina E, Curato C, Brinckmann MP, Timm M, **Grzesiak A**, Unger T, Li J. *Angiotensin AT2 receptor mediates cardiac c-kit plus cell proliferation and supports survival of cardiomyocyte*. Journal of Hypertension 26: S276-S276 Suppl. 1, 2008
7. Brinckmann MP, Timm M, Kaschina E, Altarche-Xifro W, **Grzesiak A**, Curato C, Unger T, Li J. *Cardiac estrogen receptor-alpha supports survival of cardiomyocytes through c-kit plus cells in response to ischemic injury*. Journal of Hypertension 26: S279-S279 Suppl. 1, 2008
8. Curato C, **Grzesiak A**, Kaschina E, Altarche-Xifro W, Timm M, Brinckmann MP, Unger T, Li J. *Angiotensin AT2 receptor in inflammation after myocardial infarction*. Journal of Hypertension 26: S325-S325 Suppl. 1, 2008
9. Kaschina E, **Grzesiak A**, Kemnitz UR, Kintscher U, Unger T. *Rimonabant improves the heart function in the rat with metabolic syndrome*. Journal of Hypertension 26: S342-S342 Suppl. 1, 2008
10. **Grzesiak A**, Kaschina E, Foryst-Ludwig A, Sommerfeld M, Kemnitz UR, Curato C, Timm M, Hallberg A, Li J, Steckelings UM, Unger T. *The angiotensin AT2 receptor agonist compound 21*

improves heart function after myocardial infarction in the rat by preventing apoptosis and inflammation. Hypertension 50 (4): 803-803, 2007

11. Curato C, Timm M, Brinckmann MP, **Grzesiak A**, Altarache-Xifro W, Kaschina E, Unger T, Li J. *Angiotensin receptors in inflammation after myocardial infarction. Hypertension 50 (4): 808-808, 2007*

12. Altarache-Xifro W, Birka C, Kaschina E, Curato C, Brinckmann MP, Timm M, **Grzesiak A**, Unger T, Li J. *Angiotensin AT2 receptor mediates cardiac c-kit plus cell proliferation and supports survival of cardiomyocyte. Hypertension 50 (4): 809-809, 2007*

13. Schrader F, **Grzesiak A**, Kemnitz UR, Krikov M, Sommerfeld M, Unger T, Kaschina E. *Telmisartan reduces abdominal aneurysm formation in the rat by decreasing proteolysis, apoptosis and inflammation. Hypertension 50 (4): 810-810, 2007*

14. **Grzesiak A**, Kaschina E, Curato C, Steckelings UM, Hallberg A, Li J, Unger T. *The angiotensin AT2 receptor agonist compound 21 improves heart function after myocardial infarction in the rat. Journal of Hypertension 25: S13-S13 Suppl. 2, 2007*

15. Kaschina E, Schrader F, Krikov M, Kemnitz UR, **Grzesiak A**, Sommerfeld M, Unger T. *Telmisartan protects from aneurysm formation in the rat by inhibiting proteolysis, apoptosis and inflammation. Journal of Hypertension 25: S394-S395 Suppl. 2, 2007*

16. Brinckmann M, Timm M, Kaschina E, Curato C, **Grzesiak A**, Birka C, Unger T, Li J. *ER alpha are exclusively expressed in cardiac stem cells and mediate self-renewal/differentiation after cardiac ischemic injury in rats. Hypertension 48 (4): 762-762, 2006*

17. Birka C, Kaschina E, Curato C, Brinckmann MP, Timm M, **Grzesiak A**, Unger T, Li J. *Angiotensin AT2 receptors are expressed in cardiac c-kit+ cells and mediate cell survival after myocardial infarction in rats. Dtsch Med Wochenschr 131, S151, Suppl 6, 2006*

18. Brinckmann MP, Timm M, Kaschina E, Curato C, **Grzesiak A**, Birka C, Unger T, Li J. *ER alpha is exclusively expressed in cardiac stem cells and supports self-renewal after cardiac ischemic injury in rats. Dtsch Med Wochenschr 131, S153, Suppl 6, 2006*